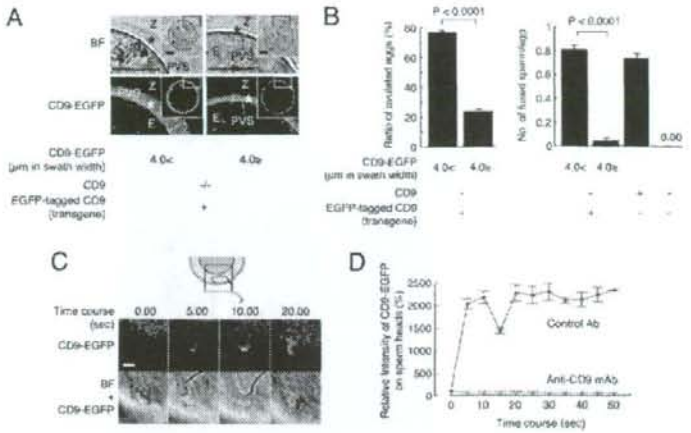

Fig. 3. Involvement of CD9-containing vesicles in sperm–egg fusion. (*A*) Categorization of $Tg^+CD9^{-/-}$ eggs (E) into two groups according to the thickness of CD9-EGFP in the PVS (*) and the inner region of the zona pellucida (Z) (>4.0 μm or ≤ 4.0 μm), indicated by double-headed lines. The boxed regions in *Insets* are enlarged. Scale bar: 20 μm. (*B*) Comparison of the fusing ability of two groups of $Tg^+CD9^{-/-}$ eggs with wild-type sperm. Left graph: Ratio of two groups of $Tg^+CD9^{-/-}$ eggs ovulated from 12 females (mean ± SEM). Right graph: Number of sperm fused per egg in two groups of zona-intact $Tg^+CD9^{-/-}$ eggs ovulated from 12 females (>4.0 μm, $n = 204$; ≤4.0 μm, $n = 66$) (mean ± SEM). $CD9^{+/+}$ ($n = 120$) and $CD9^{-/-}$ ($n = 112$) served as positive and negative controls, respectively. (*C* and *D*) Monitoring of the association of egg CD9-containing vesicles with wild-type sperm. $Tg^+CD9^{-/-}$ eggs were incubated with the sperm and monitored immediately after the sperm penetrated the zona pellucida under the presence of anti-CD9 mAb (boxed region). The values were calculated from data scanning by confocal microscopy (15 sperm in triplicate dishes) Blue: Preimmune rat IgG. Red: Anti-CD9 mAb (KMC8) (mean ± SEM). The average values of the fluorescent intensities of CD9-EGFP at 0 s were set to 100%, and the final concentration of antibodies was adjusted to 50 μg/ml. Scale bar, 5 μm.

confocal images sectioned through the largest diameter, the accumulation of CD9-EGFP from the plasma membrane to the inner region of the zona pellucida was >4.0 μm in swath width in one group and ≤ 4.0 μm in the other group. The accumulation of CD9-EGFP was predicted to show that CD9-containing vesicles are more highly accumulated within the PVS in the >4.0-μm group compared with the ≤ 4.0-μm group. Comparing the ratio of these two groups in $Tg^+CD9^{-/-}$-ovulated eggs revealed a much higher percentage of the >4.0-μm group (77.0 ± 1.3% vs.23.7 ± 1.5%) (Fig. 3*B Left*). Therefore, we focused on the heterogeneity of CD9-EGFP accumulation within the PVS and determined the ratio of the two groups in zona-intact $Tg^+CD9^{-/-}$ eggs that successfully fused with the sperm 6 h after insemination. The >4.0-μm group of $Tg^+CD9^{-/-}$ eggs showed higher activity for fusion with sperm (0.81 ± 0.04 sperm fused per egg), compared with the ≤40-μm group of $Tg^+CD9^{-/-}$ eggs (0.05 ± 0.03) and the $CD9^{-/-}$ eggs (0.00 ± 0.00), and comparable activity to that of wild-type eggs (0.73 ± 0.04) (Fig. 3*B Right*). The average activity of all $Tg^+CD9^{-/-}$ eggs (0.72 ± 0.03 sperm fused per egg) was equal to that of wild-type eggs (0.73 ± 0.04 sperm fused per egg). The difference between the two groups of $Tg^+CD9^{-/-}$ eggs was statistically significant (Fig. 3*B*). These results suggest that the quantities of CD9-containing vesicles, as assessed by the swath width of CD9-EGFP, are strongly correlated with the frequency of sperm–egg fusion.

To detect the association between sperm and CD9-containing vesicles, we serially monitored the wild-type sperm that penetrated the zona pellucida of the $Tg^+CD9^{-/-}$ eggs (Fig. 3 *C* and *D*). As shown in the diagram, we began monitoring the sperm immediately after the head portion of sperm penetrated the zona pellucida of the $Tg^+CD9^{-/-}$ eggs (Fig. 3*C Upper*, boxed area in the diagram). Soon after we began to monitor the sperm, the fluorescent intensities of CD9-EGFP on the sperm heads increased and then decreased rapidly between 0 s and 15 s, then increased again, reaching a maximum at 20 s. At this point, the CD9-EGFP fully covered the surface of the sperm heads. In contrast, when the sperm were incubated with $Tg^+CD9^{-/-}$ eggs in the medium containing anti-CD9 mAb, no increase in intensity of CD9-EGFP on the sperm heads was detected. Anti-CD9 mAbs have been reported to inhibit sperm–egg fusion (4, 15, 16). Our findings demonstrate that the anti-CD9 mAb inhibited the association of sperm with CD9-containing vesicles in parallel to inhibition of sperm–egg fusion.

To determine whether CD9-containing vesicles are capable of initiating sperm–egg fusion, we incubated the sperm with $CD9^{-/-}$ eggs in medium containing the vesicles collected from $CD9^{+/+}$ eggs (Fig. 4 and Fig. S3). To restrict the source of CD9 into the vesicles from the $CD9^{+/+}$ eggs, we used sperm collected from the epididymis of $CD9^{-/-}$ males. We estimated the capability of the vesicles to influence fusion by counting the number of sperm fused with $CD9^{-/-}$ eggs. As shown in the experimental design, after the zona pellucida was removed from the $CD9^{-/-}$ eggs, the eggs were incubated with sperm in the medium containing the vesicles (Fig. 4*A*). When examined at 1 h after incubation, the sperm were seen to be capable of fusing with $CD9^{-/-}$ eggs after co-incubation with the vesicles (Fig. 4*A Center*), indicating restoration of the fusibility of $CD9^{-/-}$ eggs with the sperm (0.58 ± 0.07 sperm fused per egg) (Fig. 4*B*). We detected further evidence of sperm–egg fusion in the $CD9^{-/-}$ eggs from which a second polar body had been extruded. In contrast, we did not detect improved fusibility of sperm with eggs in medium depleted of CD9-containing vesicles using beads conjugated with anti-CD9 mAb (Fig. 4*A Right* and *B*). After treatment with the beads, the quantity of CD9 in the depleted medium was significantly decreased, to 16% of the untreated medium (Fig. 4*C*). In addition, $CD9^{-/-}$ remnants failed to rescue the fusing ability of $CD9^{-/-}$ eggs. These findings indicate that the association with CD9-containing vesicles renders the sperm capable of fusing with eggs without endogenous CD9 expression. We estimated the relative abundance of CD9 in the remnant as 18% of the total amount in the eggs (Fig. 4*C*). We further found

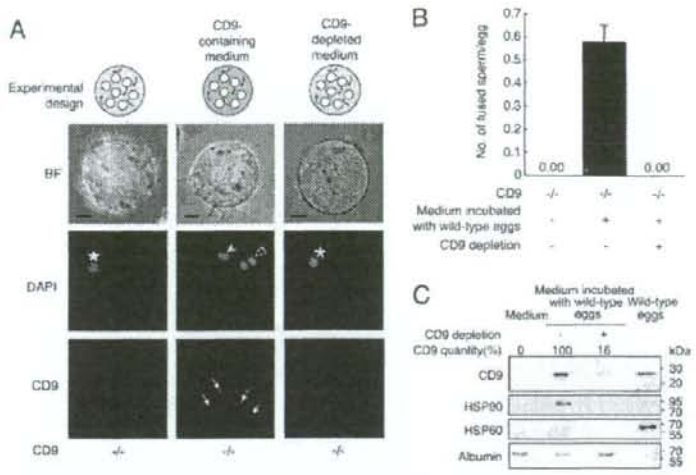

Fig. 4. Identification of fusion-facilitating activity of CD9-containing vesicles. (*A*) Estimation of the fusion-facilitating ability of the vesicles in sperm–egg fusion. As shown in the experimental design, $CD9^{-/-}$ sperm were incubated with $CD9^{-/-}$ eggs (white circles) in media containing egg-released vesicles after the zona pellucida was removed from these eggs. CD9 was detected by anti-CD9 mAb conjugated with Alexa488. The eggs were preloaded with DAPI before incubation with the sperm, to allow counting of the number of fused sperm. (*Left*) $CD9^{-/-}$ eggs at 1 h after incubation with the sperm, as a negative control. *Center* $CD9^{-/-}$ eggs cultured in the medium containing CD9 collected from wild-type eggs. (*Right*) $CD9^{-/-}$ eggs cultured in the medium depleted of CD9 by beads conjugated with anti-CD9 mAb, showing the fused sperm to eggs (arrowhead), metaphase II–arrested chromosomes (*), a second polar body (open arrowhead), and CD9 translocated on the sperm heads (arrow). The fluorescent z-series images were projected as three-dimensional images. Scale bar: 20 μm. (*B*) Number of fused sperm with the zona-free eggs counted at 1 h after incubation (mean ± SEM): $CD9^{-/-}$ eggs as a negative control (n = 51), $CD9^{-/-}$ eggs cultured in the medium containing CD9 (n = 112), and $CD9^{-/-}$ eggs cultured in the medium depleted of CD9 by antibody-conjugated beads (n = 74). The total numbers of eggs examined are in parentheses. (*C*) Western blot analysis of the media incubated with $CD9^{+/+}$ eggs for CD9, HSP90, and HSP60. Loaded samples (left to right): The medium as a negative control, the medium containing the remnant material from 40 eggs per lane (bead-untreated and -treated), and 5 eggs per lane as a positive control. The albumin contained in the medium was detected by Coomassie brilliant blue staining as an internal control. The quantities of CD9 in the media were measured densitometrically (using National Institutes of Health Image software).

that the decreased amount of CD9 after the bead treatment was synchronized with that of a cytoplasmic chaperone, HSP90 (17), but not with a mitochondrial chaperone, HSP60 (18). Our analysis of the egg-conditioned medium indicated that CD9-containing vesicles contained HSP90, a conserved component of exosomes (9, 10).

To estimate the contribution of CD9-containing vesicles to sperm–egg fusion, we examined the restoration of the impaired sperm-fusing ability in $CD9^{-/-}$ eggs co-incubated with $CD9^{+/-}$ or $CD9^{+/+}$ eggs expressing endogenous CD9 (Figs. 5 and S4*A*). We predicted that when sperm were incubated with a mixture of eggs, the vesicles released from $CD9^{+/-}$ or $CD9^{+/+}$ eggs would

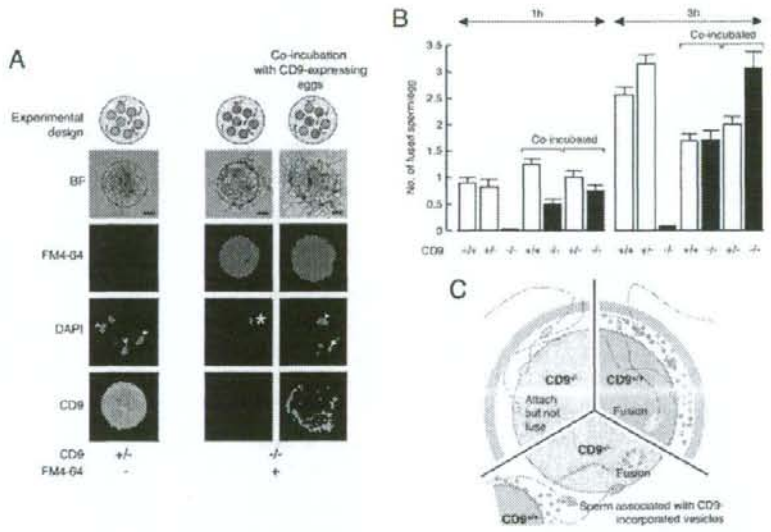

Fig. 5. Recovery of impaired fusion of $CD9^{-/-}$ eggs with sperm by CD9-containing vesicles. (*A*) Estimation of the fusion-facilitating ability of the vesicles in sperm–egg fusion. As shown in the experimental design, sperm were incubated with a mixture of CD9-expressing eggs (green circles) and $CD9^{-/-}$ eggs (red circles) after the zona pellucida was removed from these eggs. The eggs were preloaded with DAPI before incubation with sperm, to allow counting of the number of fused sperm. $CD9^{-/-}$ eggs were prestained with FM4–64 and thus were easily distinguished from CD9-expressing eggs after incubation with the sperm. (*Left*) $CD9^{+/-}$ eggs at 1 h after incubation with the sperm, as a positive control. (*Center*) $CD9^{-/-}$ eggs, as a negative control. (*Right*) $CD9^{-/-}$ eggs co-incubated with $CD9^{+/-}$ eggs, showing fused sperm to egg (arrowheads), metaphase II–arrested chromosomes (*), and extruded second polar body (arrow). The fluorescent z-series images were projected as three-dimensional images. CD9 was detected by anti-CD9 mAb conjugated with Alexa488. Scale bar: 20 μm. (*B*) Numbers of fused sperm with the zona-free eggs counted at 1 and 3 h after incubation (mean ± SEM). $CD9^{+/-}$ (1 h: n = 34; 3 h: n = 55), $CD9^{+/+}$ (1 h: n = 71; 3 h: n = 79), and $CD9^{-/-}$ eggs (1 h: n = 100; 3 h: n = 115) were separately incubated with sperm. Total number of coincubated eggs examined: $CD9^{+/-}$ eggs (n = 54) coincubated with $CD9^{-/-}$ eggs (n = 60), and $CD9^{+/+}$ eggs (n = 65) coincubated with $CD9^{-/-}$ eggs (n = 74) at 1 h; $CD9^{+/-}$ eggs (n = 51) coincubated with $CD9^{-/-}$ eggs (n = 33), and $CD9^{+/+}$ eggs (n = 98) coincubated with $CD9^{-/-}$ eggs (n = 90) at 3 h. (*C*) Schematic model of involvement of CD9-containing vesicles in sperm–egg fusion: $CD9^{+/+}$ (green), $CD9^{-/-}$ (light blue), and $CD9^{-/-}$ eggs coincubated with $CD9^{+/+}$ wild-type eggs with sperm (yellow).

interact with sperm, and these sperm could fuse with $CD9^{-/-}$ eggs. If sperm-fusing ability were regulated mainly by CD9-containing vesicles, then the number of sperm fused to $CD9^{-/-}$ eggs would be predicted to be almost equal to that fused to $CD9^{+/-}$ or $CD9^{+/+}$ eggs coincubated with $CD9^{-/-}$ eggs. We counted the number of fused sperm in coincubated CD9-expressing eggs ($CD9^{+/-}$ and $CD9^{+/+}$) and $CD9^{-/-}$ eggs. The $CD9^{-/-}$ eggs were prestained with FM4–64 (19), a fluorescent dye used to stain the membrane of live cells, and thus could be easily distinguished from the $CD9^{+/-}$ and $CD9^{+/+}$ eggs. FM4–64 did not transfer between the $CD9^{-/-}$ eggs and the $CD9^{+/-}$ or $CD9^{+/+}$ eggs. As shown in the experimental design, after the zona pellucida was removed from the eggs, $CD9^{-/-}$ eggs (red circles) were mixed with $CD9^{+/-}$ or $CD9^{+/+}$ eggs (green circles), and sperm were added to the medium containing these eggs (Fig. 5*A*). At 1 h after insemination, significant fusion of sperm with the $CD9^{-/-}$ eggs was facilitated (0.75 ± 0.11 and 0.50 ± 0.09 sperm fused per egg), corresponding to that in the $CD9^{+/-}$ (1.00 ± 0.13) and $CD9^{+/+}$ eggs (1.25 ± 0.10). At 3 h after insemination, the fusion of sperm with the $CD9^{-/-}$ eggs was restored (3.06 ± 0.30 and 1.70 ± 0.18 sperm fused per egg) to levels comparable to those in the $CD9^{+/-}$ (2.00 ± 0.15) and $CD9^{+/+}$ eggs (1.69 ± 0.13). We also detected a second polar body extruding from the $CD9^{-/-}$ eggs (Fig. 5*A Right*, arrow). In contrast, we did not observe the translocation of vesicles from the $CD9^{+/-}$ and $CD9^{+/+}$ eggs to the $CD9^{-/-}$ eggs when sperm were not added to the mixture, even after 10 h of incubation (Fig. S4*B*). These data demonstrate that the defect in the fusing ability of $CD9^{-/-}$ eggs is caused by dysfunction of the mechanism facilitating the sperm-fusing activity through CD9-containing vesicles.

To further study the involvement of CD9-containing vesicles in regulating sperm-fusing ability, we evaluated the capability of hamster eggs in sperm–egg fusion (Fig. S5). Hamster eggs have the ability to fuse with other mammalian sperm and thus are used as a tool to evaluate the fusing ability of human sperm (20). When hamster eggs were incubated with $CD9^{-/-}$ eggs after the zona pellucida was removed from these eggs, the sperm-fusing ability of these eggs was improved significantly. The sperm-fusing ability acquired through the exposure to hamster eggs was not as great as that produced by exposure to mouse eggs, probably due to the slightly different CD9 in hamster and mouse eggs (21). These results indicate that the function of CD9-containing vesicles in the acquisition of sperm-fusing ability is widely conserved in mammals.

Discussion

In sperm–egg fusion, there is a significant direct interaction between the cell membranes of sperm and eggs (1, 20, 22); however, our results demonstrate that CD9-containing vesicle–sperm interaction precedes the direct cell membrane interaction between sperm and eggs. Based on our data, we propose that the release of CD9-containing vesicles from eggs before fertilization facilitates the sperm-fusing ability that renders the sperm competent to fuse with $CD9^{-/-}$ eggs (Fig. 5*C*). Our finding of CD9-EGFP in living unfertilized eggs demonstrates that CD9-containing vesicles are present in the PVS, and that these vesicles accumulate inside the PVS during the germinal vesicle (1) and metaphase II-arrested stages (1). During this period, the egg undergoes drastic cytological changes with the increased number of microvilli (1, 22), predicting the correlation between vesicle release and microvilli formation. As expected, this correlation is supported by the finding that CD9 deficiency leads not only to impaired microvilli formation (8) (Fig. S2), but also to decreased accumulation of vesicles within the PVS. These data support the association between the release of CD9-containing vesicles from eggs and the formation of microvilli on the egg plasma membrane.

As reported previously, somatic cells are capable of releasing proteins and lipids included in membrane organelles, termed exosomes (9, 10), which are pinched out from the plasma membrane (23). Exosomes share many additional properties with retroviral particles, including similar lipid and protein compositions, such as tetraspanin (23). GM3 and HSP90 are known to be conserved components of exosomes (10). Our results show that CD9-containing vesicles released from eggs share these two components, implying that the vesicles are "exosome-like." Previous studies of macrophages have proposed that exosome biogenesis occurs only by outward budding at endosomal membranes, followed by the fusion of vesicle-laden endosomes with the plasma membrane (9, 23). If the CD9-containing vesicle were derived from exosomes and generated from the fusion of endosomes with the plasma membrane, then the vesicles would contain some proteases (9, 23), fuse with the sperm membrane, and possibly activate the sperm fusogenic factor(s) by enzymatic activities.

In hamster eggs, expansion of the PVS has been deemed essential or at least beneficial to normal fertilization (20, 21, 24), indicating that materials involved in fusion with sperm are released from eggs before fertilization in hamsters and in mice. Because anti-CD9 mAbs are not available for hamster CD9, we could not directly confirm CD9-containing vesicle release from hamster eggs before fertilization. Instead, our co-incubation assay demonstrated that hamster eggs facilitate the fusion of sperm with $CD9^{-/-}$ eggs, indicating that hamster eggs share a similar mechanism with mouse eggs through egg-released materials. Moreover, it has been reported that growing oocytes bind to sperm and transfer fluorescent dyes to the sperm head (25). At this stage, oocytes have CD9 on the cell membrane but lack CD9-containing vesicles (Fig. S1). We presume that the transfer of fluorescent dye from growing oocytes to sperm heads is mediated by CD9 on the cell membrane. Based on our findings, we propose that the CD9-containing vesicle has an ability to facilitate sperm—egg fusion. This knowledge has great potential for clinical applications, such as the induction of sperm–egg fusion using exogenous sources.

Materials and Methods

Animals. The mice that we produced were back-crossed into a C57BL/6 genetic background. Wild-type eggs were collected from C57BL/6 females (8–12 weeks old). Wild-type sperm were obtained from the epididymides of B6C3F1 males (8–12 weeks old). Hamster eggs were obtained commercially as frozen unfertilized eggs (NOSAN).

Antibodies and Chemicals. Antibodies against CD9 (KMC; BD PharMingen), beta-tubulin (Tub2.1; Sigma), HSP60 (24/HSP60; BD PharMingen), HSP90 (16F1; MBL), and GM3 (GMR6; Seikagaku) were used. Antibodies labeled with biotin by a labeling kit (Dojindo) and horseradish peroxidase-conjugated streptavidin (Sigma) were used for Western blot analysis. For immunostaining, antibodies were labeled directly with Alexa488 and Alexa546 using labeling kits (Invitrogen). FM4–64 (Invitrogen) was used to define the lipid bilayer of live eggs without disturbing sperm–egg fusion (10 μM at final concentration). We used DAPI (Invitrogen), a fluorescent dye that slowly permeates the living cell membrane (semipermeable) and slowly leaks out of cells after washing relative to Hoechst33342 (permeable), in counting the number of sperm fused per egg.

Transgenic Mice. The construct expressing mouse CD9 tagged at the N terminus with EGFP (CD9-EGFP) was subcloned into plasmid DNA-containing mouse ZP3 promoter (26). The expression cassette was excised by restriction enzyme digestion and microinjected into fertilized eggs of C57BL/6 mice, according to standard techniques (27).

Genotyping and RT-PCR. Mouse genotyping and RT-PCR were performed following standard procedures (27). (Primer sets are listed in Table S1).

Egg Collection. Eggs were collected from the oviduct 14–16 h after human chorionic gonadotropin injection (4). The eggs were placed in a drop of TYH

medium (28). Sperm collected from the epididymides were capacitated in a 100-μl drop of medium. The eggs were incubated with 1.5×10^5 sperm/ml at 37°C in 5% CO_2, and unbound sperm were washed away. The zona pellucida was removed from the eggs with acidic Tyrode's solution (4) or a piezo manipulator (11). A hole was punched through the zona pellucida with a piezo manipulator, and the eggs were removed. All materials were aspirated, including the medium but not the eggs, and used as "remnants."

Immunostaining. Zona-intact live eggs were stained with diluted antibodies in TYH medium for 30 min at 37°C, and the nonspecifically accumulated antibodies in the PVS were washed away after a brief incubation (30 min) in the medium. To measure the fluorescent intensities of GM3, three types of eggs were stained by Alexa546-labeled anti-GM3 mAb in TYH medium for 30 min, then washed in the medium for 30 min. Staining was visualized using a laser scanning confocal microscope (LSM 510 META; Carl Zeiss).

Electron-Microscopic Analysis. Live eggs were incubated with anti-CD9 mAb and anti-rat IgG mAb tagged with 5-nm gold beads. After incubation, the eggs were fixed by glutaraldehyde and osmic acid solutions. Ultra-thin sections were prepared as described in ref. 29. Eggs denuded with acid Tyrode's solution were fixed with a mixture of paraformaldehyde and glutaraldehyde and osmic acid solutions.

***In Vitro* Fertilization.** To observe the fusion with the sperm, zona-intact and zona-free eggs were incubated with DAPI (10 μg/ml) in the medium for 20 min, then washed before the sperm were added. This procedure allowed the staining of only fused sperm nuclei by dye-transfer into sperm after membrane fusion. At 1 h or 3 h after incubation in a 30-μl drop of medium, the eggs were fixed with a mixture of paraformaldehyde and glutaraldehyde for 20 min at 4°C.

Monitoring the Association of CD9-Containing Vesicles with Sperm. Eggs collected from $Tg^+CD9^{-/-}$ females were set in a 30-μl drop of TYM medium. The sperm were added to the eggs at a final concentration of 1.5×10^5/ml after incubation in the medium for 2 h. Posts of latex beads were deposited around the eggs. A glass coverslip was carefully pressed down onto the posts until the egg were fixed. The medium containing eggs and sperm was cooled to 10°C before observation. Cooling reduced the sperm motility. This procedure allowed us to measure the CD9-EGFP fluorescence on the sperm head using a confocal microscope. Images of the sperm were captured at 1 frame/s. The average value of the fluorescent intensities of CD9-EGFP at 0 s was set to 100%, and the final concentration of antibodies was adjusted to 50 μg/ml. The data are measurements of serial images from 15 wild-type sperm in triplicate dishes.

Collection of CD9-Containing Vesicles. The medium containing the vesicles was collected from denuded wild-type eggs. The eggs were cultured in a 60-μl drop of medium for 2 h after the zona pellucida was removed from the eggs. Collecting the medium containing the vesicles required an incubation time of 2 h. The collected medium was used for analysis of vesicle components and evaluation of sperm-fusing ability. CD9-depleted medium was used as a negative control. After the zona pellucida was removed from $CD9^{-/-}$ eggs, the eggs were incubated with the sperm in the medium containing CD9-incorporated vesicles for 1 h, for comparison with the vesicle-depleted medium. Details are shown in Fig. S3.

Western Blot Analysis. Quantities of proteins were examined by Western blot analysis, as described in ref. 4. As an internal loading control, quantities of albumin included in the medium were examined using Coomassie brilliant blue staining. Details are shown in Fig. S3.

Coincubation of Two Types of Eggs. $CD9^{-/-}$ eggs and CD9-expressing eggs ($CD9^{+/-}$ and $CD9^{+/+}$) were incubated in each 30-μl drop of medium after the zona pellucida was removed from these eggs. At 2 h after incubation, the $CD9^{-/-}$ eggs were added into the cultured medium of the CD9-expressing eggs. Sperm were added into the medium containing two types of eggs and incubated for 1 or 3 h. Details are shown in Fig. S4A. The frozen hamster eggs also were incubated with the $CD9^{-/-}$ eggs and wild-type sperm for 1 h. The zona pellucida of frozen hamster eggs was hardened, and removing the zona pellucida using acid Tyrode's solution took 5 min. Details are shown in Fig. S5A.

ACKNOWLEDGMENTS. This work was supported by a Precursory Research for Embryonic Science and Technology (PRESTO) grant from the Japanese Ministry of Health, Labor and Welfare and by a Grant-in-Aid for Scientific Research from the Japanese Ministry of Education, Culture, Sports, and Technology.

1. Yanagimachi R (1994) in *The Physiology of Reproduction*, eds Knobil E, Neill JD (Raven, New York), pp 189–317.
2. Kaji K, *et al.* (2000) The gamete fusion process is defective in eggs of Cd9-deficient mice. *Nat Genet* 24:279–282.
3. Le Naour F, Rubinstein E, Jasmin C, Prenant M, Boucheix C (2000) Severely reduced female fertility in CD9-deficient mice. *Science* 287:319–321.
4. Miyado K, *et al.* (2000) Requirement of CD9 on the egg plasma membrane for fertilization. *Science* 287:321–324.
5. Hemler ME (2003) Tetraspanin proteins mediate cellular penetration, invasion, and fusion events and define a novel type of membrane microdomain. *Annu Rev Cell Dev Biol* 19:397–422.
6. Barraud-Lange V, Naud-Barriant N, Bomsel M, Wolf J-P, Ziyyat A (2007) Transfer of oocyte membrane fragments to fertilizing spermatozoa. *FASEB J* 21:3446–3449.
7. Joly E, Hudrisier D (2003) What is trogocytosis and what is its purpose? *Nat Immunol* 4:815.
8. Runge K-E, *et al.* (2007) Oocyte CD9 is enriched on the microvillar membrane and required for normal microvillar shape and distribution. *Dev Biol* 304:317–325.
9. Trajkovic K, *et al.* (2008) Ceramide triggers budding of exosome vesicles into multivesicular endosomes. *Science* 319:1244–1247.
10. Wubbolts R, *et al.* (2003) Proteomic and biochemical analyses of human B cell-derived exosomes: Potential implications for their function and multivesicular body formation. *J Biol Chem* 278:10963–10972.
11. Yamagata K, *et al.* (2002) Sperm from the calmegin-deficient mouse have normal abilities for binding and fusion to the egg plasma membrane. *Dev Biol* 250:348–357.
12. Mitsuzuka K, Handa K, Satoh M, Arai Y, Hakomori S (2005) A specific microdomain ("glycosynapse 3") controls phenotypic conversion and reversion of bladder cancer cells through GM3-mediated interaction of alpha3beta1 integrin with CD9. *J Biol Chem* 280:35545–35553.
13. Yamashita T, *et al.* (2003) Enhanced insulin sensitivity in mice lacking ganglioside GM3. *Proc Natl Acad Sci USA* 100:3445–3449.
14. Kotani M, Ozawa H, Kawashima I, Ando S, Tai T (1992) Generation of one set of monoclonal antibodies specific for a-pathway ganglio-series gangliosides. *Biochim Biophys Acta* 1117:97–103.
15. Chen MS, *et al.* (1999) Role of the integrin-associated protein CD9 in binding between sperm ADAM 2 and the egg integrin alpha6beta1: Implications for murine fertilization. *Proc Natl Acad Sci USA* 96:11830–11835.
16. Miller B-J, Georges-Labouesse E, Primakoff P, Myles D-G (2000) Normal fertilization occurs with eggs lacking the integrin alpha6beta1 and is CD9-dependent. *J Cell Biol* 149:1289–1296.
17. Callahan M-K, Garg M, Srivastava P-K (2008) Heat-shock protein 90 associates with N-terminal extended peptides and is required for direct and indirect antigen presentation. *Proc Natl Acad Sci USA* 105:1662–1667.
18. Cheng M-Y, Hartl F-U, Horwich A-L (1990) The mitochondrial chaperonin hsp60 is required for its own assembly. *Nature* 348:455–458.
19. Bolte S, *et al.* (2004) FM-dyes as experimental probes for dissecting vesicle trafficking in living plant cells. *J Microsc* 214:159–173.
20. Yanagimachi R, Yanagimachi H, Rogers B-J (1976) The use of zona-free animal ova as a test system for the assessment of the fertilizing capacity of human spermatozoa. *Biol Reprod* 15:471–476.
21. Ponce R-H, Yanagimachi R, Urch U-A, Yamagata T, Ito M (1993) Retention of hamster oolemma fusibility with spermatozoa after various enzyme treatments: A search for the molecules involved in sperm–egg fusion. *Zygote* 1:163–171.
22. Primakoff P, Myles D-G (2002) Penetration, adhesion, and fusion in mammalian sperm–egg interaction. *Science* 296:2183–2185.
23. Booth A-M, *et al.* (2006) Exosomes and HIV Gag bud from endosome-like domains of the T cell plasma membrane. *J Cell Biol* 172:923–935.
24. Okada A, Yanagimachi R, Yanagimachi H (1986) Development of a cortical granule-free area of cortex and the perivitelline space in the hamster oocyte during maturation and following ovulation. *J Submicrosc Cytol* 18:233–247.
25. Zuccotti M, Yanagimachi R, Yanagimachi H (1991) The ability of hamster oolemma to fuse with spermatozoa: Its acquisition during oogenesis and loss after fertilization. *Development* 112:143–152.
26. Rankin T-L, *et al.* (1998) Human ZP3 restores fertility in Zp3 null mice without affecting order-specific sperm binding. *Development* 125:2415–2424.
27. Hogan B, Costantini F, Lacy E (1986) in *Manipulating the Mouse Embryo* (Cold Spring Harbor Lab Press, Cold Spring Harbor, NY), pp 217–252.
28. Toyoda Y, Chang M-C (1974) Capacitation of epididymal spermatozoa in a medium with high K-Na ratio and cyclic AMP for the fertilization of rat eggs in vitro. *J Reprod Fertil* 36:125–134.
29. Toshimori K, Saxena D-K, Tanii I, Yoshinaga K (1998) An MN9 antigenic molecule, equatorin, is required for successful sperm–oocyte fusion in mice. *Biol Reprod* 59:22–29.

Conjoined twins in a triplet pregnancy after intracytoplasmic sperm injection and blastocyst transfer: case report and review of the literature

Tetsuya Hirata, M.D., Ph.D, Yutaka Osuga, M.D., Ph.D, Akihisa Fujimoto, M.D., Ph.D, Hajime Oishi, M.D., Ph.D, Hisahiko Hiroi, M.D., Ph.D, Toshihiro Fujiwara, M.D., Ph.D, Tetsu Yano, M.D., Ph.D, and Yuji Taketani, M.D., Ph.D.

Department of Obstetrics and Gynecology, Faculty of Medicine, University of Tokyo, Tokyo, Japan

Objective: To describe an exceptional case of conjoined twins in a triplet pregnancy after intracytoplasmic sperm injection (ICSI) and blastocyst transfer.
Design: Case report.
Setting: University teaching hospital reproductive endocrinology department and infertility practice.
Patient(s): A 34-year-old woman underwent ICSI and received two blastocysts transferred.
Intervention(s): Transvaginal ultrasonography performed sequentially during early pregnancy.
Main Outcome Measure(s): Ultrasound images of the fetus in gestational sac.
Result(s): Two gestational sacs in the uterus were revealed at the 5th week. At the 8th week of gestation, a single fetus was seen in one sac, whereas thoracopagus conjoined twins was diagnosed in the other sac. At the 10th week, the conjoined twins had a spontaneous cardiac arrest confirmed by color Doppler. The subsequent course was uneventful, and a healthy child was born at 39th week.
Conclusion(s): To date, a small number of cases of conjoined twins in IVF/ICSI pregnancies have been reported, in which most cases were treated with manipulations causing possible trauma in the zona pellucida. Our case is unique in that the transferred embryos were blastocysts that might have had additional damage on the zona pellucida from the longer culture. (Fertil Steril® 2008;■:■–■. ©2008 by American Society for Reproductive Medicine.)

Key Words: Conjoined twins, triplet pregnancy, ICSI, blastocyst transfer, ultrasound

Conjoined twins (CT) are identical twins whose bodies are joined in utero. It is a rare phenomenon, estimated to range from 1 in 200,000 to 1 in 100,000 live births (1). Although the precise etiology of the disease remains to be elucidated, CT result from an abnormal process during the development of monozygotic twins (MZT) and make up about 1% of MZT (2).

As assisted reproduction technologies (ART) have become widely used all over the world to treat infertility, several kinds of techniques to micromanipulate the embryo have been developed. Blastocyst transfer is a technique that can simultaneously maintain high pregnancy rates and prevent higher-order multiple gestation by limiting the number of embryos to transfer (3). However, several reports show that blastocyst transfer is related to a higher incidence of MZT (4–6), implying that the procedure might also enhance the frequency of CT.

In the present report, we present a case of CT in a triplet pregnancy conceived after intracytoplasmic sperm injection (ICSI) and subsequent blastocyst transfer into the uterus. We also reviewed the literature reporting the cases of CT after ART procedure.

Received June 13, 2008; revised July 2, 2008; accepted July 9, 2008.
T.H. has nothing to disclose. Y.O. has nothing to disclose. A.F. has nothing to disclose. H.O. has nothing to disclose. H.H. has nothing to disclose. T.F. has nothing to disclose. T.Y. has nothing to disclose. Y.T. has nothing to disclose.
Reprint requests: Yutaka Osuga, Department of Obstetrics and Gynecology, Faculty of Medicine, University of Tokyo, 7-3-1, Hongo, Bunkyo-ku, Tokyo, 113-8655, Japan (FAX: +81-3-3816-2017; E-mail: yutakaos-tky@umin.ac.jp).

CASE REPORT

A 34-year-old gravida 1 para 1 woman underwent ovulation induction followed by ICSI and embryo replacement. Her husband's sperm analysis showed asthenozoospermia. Her previous pregnancy was achieved by ICSI and day 3 embro transfer (ET). A healthy baby was delivered vaginally at the 37th week of gestation. Her family history and past medical history were unremarkable.

Before starting ovulation induction, pituitary down-regulation was achieved by daily use of a GnRH agonist (nafarelin acetate; Nasanyl; Astellas, Tokyo, Japan) administered at the midluteal phase of the previous cycle (day 9 after ovulation). At day 14 after ovulation, menstruation was confirmed. Then, ovulation induction was performed by daily injections of hMG (Humegon; Organon Japan, Tokyo, Japan) starting on day 5 of the menstrual cycle. After 14 days of the gonadotropin administration (total 1,500 IU), oocyte maturation was triggered by injecting 10,000 IU hCG (Mochida Pharmaceutical Co., Osaka, Japan). At that time, the serum E_2 level was 1,793.3 pg/mL.

Transvaginal oocyte retrieval was performed under sonographic guidance 34 h after hCG administration. Twenty-one

0015-0282/08/$34.00 Fertility and Sterility® Vol. ■, No. ■, ■ 2008 1.e1
doi:10.1016/j.fertnstert.2008.07.1730

FIGURE 1

Microscopic view of the blastocysts transferred: early blastocyst and 4BB by Gardner's blastocyst evaluation criteria.

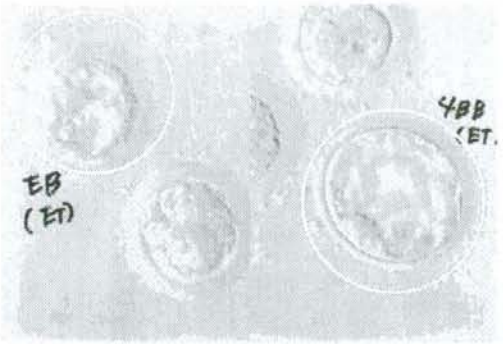

Hirata. Conjoined twins after ART. Fertil Steril 2008.

oocytes were retrieved. Fifteen oocytes were mature (metaphase II) and considered to be suitable for insemination by the ICSI procedure. Thirteen oocytes were fertilized and incubated in cleavage medium (IVC-two; In Vitro Care, San Diego, CA) with 10% human serum albumin. From day 3 after ICSI, all embryos were cultured in sequential media (Sydney IVF Blast Medium; Cook, Brisbane, Australia). Two blastocysts (early blastocyst and 4BB by Gardner's blastocyst evaluation criteria (7)) were obtained and transferred to the uterus on day 5 (Fig. 1). Luteal support was given by administration of 1.44 mg transdermal E_2 patch (Estraderm M; Novartis, Basel, Switzerland) every other day and transvaginal suppository of 200 mg P every day.

Nine days after ET, serum hCG level was 285.0 mIU/mL. At 5 weeks and 3 days of gestation, transvaginal sonography revealed two gestational sacs in the uterus. Transvaginal sonography was thereafter performed at weekly intervals. At 6 weeks 5 days of gestation, a single fetal heartbeat was detected in each of the gestational sac. At the 8th week of gestation, a fetus, with a crown-rump length of 13.5 mm, was seen in one sac, and inseparable fetal bodies were seen in the other sac (Fig. 2). The two fetuses had two separate skulls and were joined at the thorax with a common heart. The conjoined fetuses were diagnosed as thoracopagus twins, and by means of color Doppler, a single beating heart shared between the thoraxes was demonstrated. At 10 weeks 3 days of gestation, the CT had a spontaneous cardiac arrest confirmed by means of color Doppler.

The subsequent prenatal course was uneventful. A normal healthy child was born at the 39th week of gestation by spontaneous vaginal delivery (weight 2,792 g, male). Vestiges of the CT could not be detected in the appendages.

DISCUSSION

To our knowledge, the present case is the first report of CT occurring in a triplet pregnancy after transfer of two blastocysts obtained by ICSI procedure. Although the origins of CT remain unknown, CT are generally considered to be a variant of MZT. Two theories have been proposed to explain the origins of CT (8). "Fission theory" proposes the incomplete separation of embryonic discs at around 13 to 15 days after fertilization. "Fusion theory" postulates that secondary fusion occurs between two originally separate embryonic discs (9).

As ART has become one of the popular methods to treat infertility all over the world, reported cases of MZT have increased (4, 5, 10, 11). It has been suggested that steps in ART, such as ovulation induction (11), conventional IVF, ICSI, blastocyst culture (4, 5), and assisted hatching (10) may have increased the occurrence of MZT. Similarly, the incidence of CT could be increased by ART. However, because CT are very rare phenomenon, we do not have enough epidemiologic data to understand the true occurrence of CT after ART.

FIGURE 2

Ultrasonographic image of the conjoined twins in a triplet pregnancy. Single fetus (**A**) and conjoined twins (**B**) at 8.0 weeks' gestation.

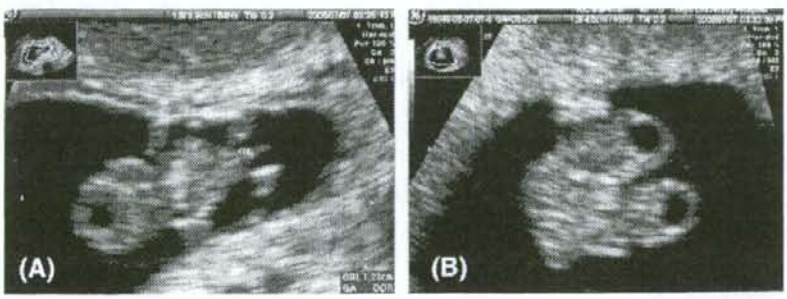

Hirata. Conjoined twins after ART. Fertil Steril 2008.

TABLE 1

Reported cases of conjoined twins after assisted reproduction.

Case no.	Age	Gravity	Parity	Day of embryo transfer	Type of cycle	Treatment	Assisted hatching	No. of embryos transferred	No. of gestational sacs	No. of fetuses	Gestational age at disgnosis of CTs	Selective termination	No. of newborns	Result	Author
1	27	ND	0	ND	Fresh	IVF	–	2	2	3	10w	+	1	NVD	Boulot et al. (13)
2	35	ND	2	Day 3	Fresh	IVF	+	4	2	3	12w	+	1	Ongoing in the third trimester	Skupski et al. (18)
3	28	1	0	ND	Fresh	ICSI	–	3	2	3	8w4d	+	1	NVD (37w)	Goldberg et al. (15)
4	30	0	0	Day 3	FET	ICSI	+	2	2	3	10w	–	1	Abortion (12w), NVD (38w)	Sugawara et al. (19)
5	37	2	1	ND	FET	ICSI	–	4	3	4	11w3d	+	1	Elective C/S (38W)	Maymon et al. (16)
6	38	0	0	Day3	Fresh	ICSI	+	3	3	4	11w3d	+	2	Elective C/S (38w)	Allegra et al. (12)
7	36	0	0	Day 3 and 5	Fresh	IVF	–	3	1	2	10w	NA	0	Termination (11w)	Shimizu et al (17)
8	30	2	0	ND	Fresh	ICSI	–	2	1	2	28w	NA	1	C/S (30w, neonatal death)	Fujimori et al. (14)

Note: Cases 1–6 is in quadruplet or triplet pregnancy. Cases 7 and 8 were single gestational sac. C/S = cesarean section; FET = frozen-thawed embryo transfer; ICSI = intracytoplasmic sperm injection; NA = not applicable; ND = not documented; NVD = vaginal delivery.

Hirata. Conjoined twins after ART. Fertil Steril 2008.

To date, eight cases of CT after ART have been previously reported in the literature (Table 1) (12–19). A notable finding is that seven (including the present case) out of nine cases of CT involved ICSI or assisted hatching (AHA): four cases with ICSI, one case with AHA, and 2 cases with both ICSI and AHA. These techniques introduce small openings or thin areas in the zona pellucida that may cause herniation of the embryo through these defects. The embryo may also get pinched off and divide, forming identical twins and contributing to the development of CT. This has also been suggested to explain the higher rate of MZT that occurs after zona manipulation (20), such as ICSI (21, 22) and AHA (10, 23).

The zona pellucida may also be susceptible to in vitro culture conditions. Prolonged in vitro culture may harden the zona pellucida, contributing to the formation of MZT (10). Supporting evidence indicates that a high rate of MZT occurred after blastocyst stage transfer compared with day 3 embryo transfer (4–6). Regarding CT, to our knowledge there is only one earlier report in the literature documenting CT derived from blastocyst transfer (Table 1, case 7). However, in that case, it is unclear whether CT were derived from blastocyst or from day 3 embryos, because they report a unique technique in which two-step embryo transfer was performed. Therefore, we believe the present case is the first report of CT derived from blastocyst transfer.

The incidence of monozygotic splitting in pregnancies with two or more gestational sacs has been reported to be higher than that of pregnancies with a single gestational sac (5, 11). Similarly, the incidence of CT may increase in pregnancies with two or more gestational sacs than with a single gestational sac. Although we have very few published case reports available, supporting evidence indicates that two out of nine cases of CT were derived from a single gestational sac, whereas seven out of nine cases of CT were derived from two or three gestational sacs.

The present case was diagnosed by transvaginal sonography at 8.0 weeks' gestation, earlier than any other cases previously reported. The early diagnosis of CT by careful sonography permits the choice of selective termination in triplet or more pregnancy of different chorionicity. However, we did not know the best timing for selective termination, because the incidence of spontaneous abortion in conjoined twins is unknown. In this case, the conjoined twins had spontaneous cardiac arrest at 10 weeks 3 days of gestation. As shown in Table 1, it has been reported that irrespective of selective termination or spontaneous abortion of CTs, the subsequent course of residual viable fetus was uneventful.

In conclusion, to our knowledge, we report the first case of CT in a triplet pregnancy after ICSI and blastocyst transfer. Review of the literature and the present case suggests that ART might increase the incidence of CT, possibly owing to the manipulation of the zona pellucida. More research is needed to understand the mechanisms by which CT are formed with blastocyst transfer.

Acknowledgments: The authors thank Dr. Mieko Fukui for her assistance in editing the manuscript and Dr. Nagisa Ooi for her technical assistance.

REFERENCES

1. Rees AE, Vujanic GM, Williams WM. Epidemic of conjoined twins in Cardiff. Br J Obstet Gynaecol 1993;100:388–91.
2. Maggio M, Callan NA, Hamod KA, Sanders RC. The first-trimester ultrasonographic diagnosis of conjoined twins. Am J Obstet Gynecol 1985;152:833–5.
3. Gardner DK, Schoolcraft WB, Wagley L, Schlenker T, Stevens J, Hesla J. A prospective randomized trial of blastocyst culture and transfer in in-vitro fertilization. Hum Reprod 1998;13:3434–40.
4. da Costa ALA, Abdelmassih S, de Oliveira FG, Abdelmassih V, Abdelmassih R, Nagy ZP, et al. Monozygotic twins and transfer at the blastocyst stage after ICSI. Hum Reprod 2001;16:333–6.
5. Milki AA, Jun SH, Hinckley MD, Behr B, Giudice LC, Westphal LM. Incidence of monozygotic twinning with blastocyst transfer compared to cleavage-stage transfer. Fertil Steril 2003;79:503–6.
6. Sheiner E, Har-Vardi I, Potashnik G. The potential association between blastocyst transfer and monozygotic twinning. Fertil Steril 2001;75:217–8.
7. Gardner DK, Schoolcraft WB. In vitro culture of the human blastocysts. In: Jansen R, Mortimer D, eds. Towards reproductive certainty: infertility and genetics beyond 1999. Carnforth: Parthenon Press, 1999:378–88.
8. Spitz L, Kiely EM. Conjoined twins. JAMA 2003;289:1307–10.
9. Spencer R. Theoretical and analytical embryology of conjoined twins: part I: embryogenesis. Clin Anat 2000;13:36–53.
10. Alikani M, Noyes N, Cohen J, Rosenwaks Z. Monozygotic twinning in the human is associated with the zona pellucida architecture. Hum Reprod 1994;9:1318–21.
11. Derom C, Vlietinck R, Derom R, Van den BH, Thiery M. Increased monozygotic twinning rate after ovulation induction. Lancet 1987;1:1236–8.
12. Allegra A, Monni G, Zoppi MA, Curcio P, Marino A, Volpes A. Conjoined twins in a trichorionic quadruplet pregnancy after intracytoplasmic sperm injection and quarter laser-assisted zona thinning. Fertil Steril 2007;87: 189–12.
13. Boulot P, Deschamps F, Hedon B, Laffargue F, Viala JL. Conjoined twins associated with a normal singleton: very early diagnosis and successful selective termination. J Perinat Med 1992;20:135–7.
14. Fujimori K, Shiroto T, Kuretake S, Gunji H, Sato A. An omphalopagus parasitic twin after intracytoplasmic sperm injection. Fertil Steril 2004;82:1430–2.
15. Goldberg Y, Ben Shlomo I, Weiner E, Shalev E. First trimester diagnosis of conjoined twins in a triplet pregnancy after IVF and ICSI: case report. Hum Reprod 2000;15:1413–5.
16. Maymon R, Mendelovic S, Schachter M, Ron-El R, Weinraub Z, Herman A. Diagnosis of conjoined twins before 16 weeks' gestation: the 4-year experience of one medical center. Prenat Diagn 2005;25:839–43.
17. Shimizu Y, Fukuda J, Sato W, Kumagai J, Hirano H, Tanaka T. First-trimester diagnosis of conjoined twins after in-vitro fertilization-embryo transfer (IVF-ET) at blastocyst stage. Ultrasound Obstet Gynecol 2004;24:208–9.
18. Skupski DW, Streltzoff J, Hutson JM, Rosenwaks Z, Cohen J, Chervenak FA. Early diagnosis of conjoined twins in triplet pregnancy after in vitro fertilization and assisted hatching. J Ultrasound Med 1995;14:611–5.
19. Sugawara N, Yanagida K, Maeda M, Suzuki N, Tokunaga Y, Sato A. Conjoined twin in triplet pregnancy occurring after ICSI, cryopreservation and assisted hatching. J Mamm Ova Res 2003;20:41–4.
20. Slotnick RN, Ortega JE. Monoamniotic twinning and zona manipulation: a survey of U.S. IVF centers correlating zona manipulation procedures and high-risk twinning frequency. J Assist Reprod Genet 1996;13:381–5.
21. Abusheikha N, Salha O, Sharma V, Brinsden P. Monozygotic twinning and IVF/ICSI treatment: a report of 11 cases and review of literature. Hum Reprod Update 2000;6:396–403.
22. Tarlatzis BC, Qublan HS, Sanopoulou T, Zepiridis L, Grimbizis G, Bontis J. Increase in the monozygotic twinning rate after intracytoplasmic sperm injection and blastocyst stage embryo transfer. Fertil Steril 2002;77:196–8.
23. Hershlag A, Paine T, Cooper GW, Scholl GM, Rawlinson K, Kvapil G. Monozygotic twinning associated with mechanical assisted hatching. Fertil Steril 1999;71:144–6.

Expression and possible implication of growth hormone–releasing hormone receptor splice variant 1 in endometriosis

Li Fu, Ph.D., M.D.,[a] *Yutaka Osuga, Ph.D., M.D.,*[a] *Tetsu Yano, Ph.D., M.D.,*[a] *Yuri Takemura, Ph.D., M.D.,*[a] *Chieko Morimoto, Ph.D., M.D.,*[a] *Yasushi Hirota, Ph.D., M.D.,*[a] *Andrew V. Schally, Ph.D., M.D.h.c.,*[b] *and Yuji Taketani, Ph.D., M.D.*[a]

[a] Department of Obstetrics and Gynecology, Faculty of Medicine, University of Tokyo, Tokyo, Japan; and [b] Endocrine, Polypeptide and Cancer Institute, Veterans Affairs Medical Center, Miami, and University of Miami, Miller School of Medicine, Miami, Florida

Objective: To determine possible involvement of splice variant 1 (SV1), a variant of the pituitary growth hormone-releasing hormone (GHRH) receptor, in the development of endometriosis.
Design: Comparative and laboratory study.
Setting: University teaching hospital reproductive endocrinology and infertility practice.
Patient(s): Eutopic and ectopic endometrial tissues, and peritoneal bone marrow-derived cells were collected from women with or without endometriosis. Normal ovarian tissues were collected from women without endometriosis.
Intervention(s): Ectopic endometrial stromal cells (ESC) were isolated and cultured with or without GHRH.
Main Outcome Measure(s): Gene expression of *GHRH* and *SV1* in the sample tissues was determined by reverse transcriptase (RT) nested polymerase chain reaction (PCR). Cyclic adenosine monophosphate (cAMP) production and 5-bromo-2'-deoxyuridine (BrdU) incorporation in ESC were measured using specific assay systems.
Result(s): We detected *SV1* messenger RNA (mRNA) in 17 out of 27 (63%) ectopic endometrial tissues, which was statistically significantly higher than that detected in eutopic endometrial tissues (2 out of 47, 4%) and normal ovarian tissues (0 out of 14). A relatively low rate of *GHRH* mRNA was detected in ectopic endometrial tissues (6 out of 27, 24%) and in eutopic endometrial tissues (12 out of 47, 26%). In contrast, relatively high rates were detected in normal ovarian tissues (14 out of 14, 100%) and peritoneal bone marrow-derived cells (13 out of 16, 81%). We found that GHRH stimulated the production of cAMP and the incorporation of BrdU in SV1-expressing ESC.
Conclusion(s): GHRH and SV1 may play a role in promoting the development of endometriosis. (Fertil Steril® 2008;■:■–■. ©2008 by American Society for Reproductive Medicine.)

Key Words: Endometriosis, GHRH, SV1, proliferation

Endometriosis, defined as the presence of endometrium-like tissues outside the uterus, is one of the most common benign gynecologic disorders. The most widely accepted etiology of the disease is that endometrial tissues in retrograde menstrual flux implant and grow in the peritoneum. However, ectopic endometrium differs from eutopic endometrium, as demonstrated by gene expression analysis (1, 2). The specific characteristics of ectopic endometrium and the local environment surrounding it have been suggested to play important roles in the development of endometriosis.

Growth hormone-releasing hormone (GHRH), a peptide hormone of 42–44 amino acids, was originally thought to be secreted in the hypothalamus and to exert its actions on the pituitary gland. It is a well-established fact that GHRH stimulates the synthesis and secretion of growth hormone and regulates the proliferation and differentiation of pituitary somatotrophs (3). It is interesting that GHRH expression has also been demonstrated in normal human extrapituitary tissues and various tumors, suggesting a broader biological role for this peptide (4). An accumulating body of evidence indicates that GHRH functions as an autocrine growth factor for many neoplasms (5–7). The mitogenic effect of GHRH is mediated by a protein encoded by splice variant 1 (SV1), a splice variant of the GHRH receptor, which is highly similar to the pituitary GHRH receptor (8–14). Binding of GHRH to SV1 can stimulate adenylate cyclase to produce cyclic adenosine monophosphate (cAMP), a common secondary messenger of the pituitary GHRH receptor (8, 10, 13, 15).

We had reported previously that gonadotropin-releasing hormones (GnRH) may play a role as local regulators in the development of endometriosis (16). Others have also shown that corticotrophin-releasing hormone may be involved locally in the progression of the disease (17). These findings imply that hypothalamic hormones are involved in the pathogenesis of endometriosis. It is interesting that the expression of *GHRH* mRNA has been detected in normal endometrial tissue

Received February 28, 2008; revised and accepted April 21, 2008.
L.F. has nothing to disclose. Y.O. has nothing to disclose. T.Y. has nothing to disclose. Y.T. has nothing to disclose. C.M. has nothing to disclose. Y.H. has nothing to disclose. A.V.S. has nothing to disclose. Y.T. has nothing to disclose.
Study partly supported by grants from the Ministry of Health, Labour and Welfare, and the Ministry of Education, Culture, Sports, Science and Technology.
Reprint requests: Yutaka Osuga, Ph.D., M.D., Department of Obstetrics and Gynecology, Faculty of Medicine, University of Tokyo, 7-3-1, Hongo, Bunkyo-ku, Tokyo, 113-8655, Japan (FAX: +81-3-3816-2017; E-mail: yutakaos-tky@umin.ac.jp).

0015-0282/08/$34.00
doi:10.1016/j.fertnstert.2008.04.048

(18, 19), although the implication of this finding remains to be elucidated. We therefore speculated that GHRH might stimulate the progression of endometriosis in a similar way to that observed in many tumors that express SV1. In this study, we first explored the messenger RNA (mRNA) expression patterns of *GHRH* and the different splice variants of the *GHRH* receptor in eutopic and ectopic endometrial tissues. Then we used a primary culture system to evaluate the effects of GHRH on cAMP production in ectopic endometrial stromal cells (ESC) and on the proliferation of ESC.

MATERIALS AND METHODS

Sample Collection

We collected ectopic endometrial tissues from the walls of ovarian endometriomas from 27 women (age range: 36.4 ± 7.0 years, mean ± SD) during laparoscopic surgery. Peritoneal fluid was aspirated from the pouch of Douglas immediately after insertion of the trocar to minimize contamination with blood. Eutopic endometrial tissues were also sampled during the operations. All of the patients had regular menstrual cycles. None had received hormone treatment in the 6 months preceding surgery or had undergone previous ovarian surgeries. According to the revised American Society for Reproductive Medicine classification of endometriosis, all of the women with endometriosis were classified as stages III/IV. For the control samples, normal endometrial tissues were collected from women (age range: 34.4 ± 7.9 years) with uterine fibroids without deformity of the endometrial cavity (n = 10), ovarian dermoid cysts (n = 8), or ovarian simple cyst (n = 2). Thirteen samples were obtained during the proliferative phase and 14 samples during the secretory phase in the endometriosis group, and 9 samples were obtained during the proliferative phase and 11 samples during the secretory phase in the control group. The days of menstrual cycle when the samples were taken were distributed similarly between the groups. Additional control samples were also collected and included normal ovarian tissues from 14 women (age range: 32.7 ± 8.9 years) undergoing laparoscopic ovarian cystectomy for dermoid cysts; after complete removal of the dermoid cysts, samples of normal ovarian tissue were obtained from the ovaries. Informed written consent for the use of the specimens was obtained from each patient, and consent forms and experimental protocols were approved by the University of Tokyo's institutional review board.

Ectopic endometrial tissues obtained for cell culture were placed in Dulbecco minimal essential medium (DMEM)/F12 medium (GIBCO-BRL/Invitrogen, Grand Island, NY) on ice and transported to the laboratory immediately. Eutopic and ectopic endometrial tissues and ovarian tissues obtained for reverse transcriptase polymerase chain reaction (RT-PCR) analysis were snap-frozen in liquid nitrogen immediately after sampling and stored at −80°C.

Isolation and Purification of Peritoneal Bone Marrow–Derived Cells

Grossly hemorrhagic peritoneal fluid specimens were discarded. Peritoneal bone marrow–derived cells were collected using a method previously described elsewhere (20), in which more than 90% of the cells stained positive for mouse monoclonal anti-human CD45 (leukocyte common antigen). Briefly, the collected peritoneal fluid was centrifuged at 200 × *g* for 5 minutes, and after the supernatant was removed, the cell pellet was resuspended in phosphate-buffered saline (PBS), layered onto Ficoll-Paque (Amersham Biosciences, Piscataway, NJ) and centrifuged at 150 × *g* for 30 minutes. Peritoneal bone marrow–derived cells were recovered from the interface.

Isolation and Culture of Human ESC

We purified ESC from ovarian endometriotic tissues and cultured them as described previously elsewhere (21, 22). The fresh endometriotic lesions were collected in sterile medium and dissected away from the underlying parenchyma. Approximately 1.0 to 1.5 g of the tissue was then minced into small pieces and incubated in DMEM/F12 (GIBCO-BRL) with 2.5 mg/mL type I collagenase (Sigma, St Louis, MO) and 15 U/mL deoxyribonuclease I (Takara, Tokyo, Japan) for 2 hours at 37°C with agitation. The resulting suspension was separated by serial filtration. Debris was removed with a 100-μm nylon cell strainer (Becton Dickinson, Franklin Lakes, NJ), and some epithelial glands were eliminated with a 70-μm nylon cell strainer (Becton Dickinson). Stromal cells remaining in the filtrate were collected by centrifugation, resuspended in DMEM/F12, plated onto 100-mm dishes (Iwaki, Chiba, Japan) and allowed to adhere at 37°C for 30 minutes, after which nonadhering epithelial cells and blood cells were removed with PBS rinses. The cells were cultured in DMEM/F12 supplemented with 10% charcoal-stripped fetal bovine serum (Hyclone, Logan, UT) and antibiotics (Sigma). The purity of the ESC population was greater than 95%, as confirmed by positive immunocytochemical staining for vimentin. When the cells reached confluence, they were used for experiments at the first passage.

RT-nested PCR for Detection of GHRH and Splice Variants (SVs) of the GHRH Receptor

Total RNA was extracted from tissues and cells using the RNeasy Mini Kit (Qiagen, Hilden, Germany). One microgram of total RNA in a total volume of 20 μL was reverse transcribed and then amplified using the ReverTra Dash RT-PCR kit (Toyobo, Osaka, Japan) following the manufacturer's protocol. Gene-specific primers were synthesized by Sigma Genosys, and the sequences are listed in Table 1. To investigate the existence of *GHRH* receptor SVs and to improve the specificity and sensitivity of amplification, nested PCR was carried out as described previously elsewhere (14). For *GHRH* receptor SVs, a primary amplification using primers I3-1 and E12 (0.3 μM each) was performed using the following cycling conditions: 94°C for 5 minutes followed by 30 cycles consisting of 94°C for 30 seconds, 60°C for 2 seconds, and 74°C for 70 seconds. Subsequently, 2 μL of the primary PCR product was were used as the DNA template for the secondary PCR, using the primers I3-2 and E8 (0.3 μM each) and

TABLE 1

Human *GHRH* receptor and *GHRH* gene-specific primers used in RT-nested PCR analysis.

mRNA	Primer name[a]	Direction	Location in cDNA	Sequence (5′–3′)	Product size (bp)
GHRH receptor	I3-1	Sense		CCT ACT GCC CTT AGG ATG CTG G	
	E12	Antisense	1156–1177	GCA GTA GAG GAT GGC AAC AAT G	
	I3-2	Sense		GCA CCT TTG AAG CCA GAG AAG G	[b]
	E8	Antisense	806–827	CAC GTG CCA GTG AAG AGC ACG G	
GHRH	E1	Sense	51–70	ATT TGA GCA GTG CCT CGG AG	
	E4-1	Antisense	352–371	TTT GTT CTG CCC ACA TGC TG	
	E3	Sense	207–228	ATG CAG ATG CCA TCT TCA CCA A	150
	E4-2	Antisense	336–356	TGC TGT CTA CCT GAC GAC CAA	

[a] The primers were named according to the location of their sequences in the respective gene (e.g., primer I3 is in intron 3, and E12 is in exon 12). Splice variants possess retained intronic sequence at their 5′ end.

[b] Expected product sizes of SV1, SV2, SV3, and SV4 were 720, 556, 390, and 335 bp, respectively.

Fu. GHRH receptor SV1 in endometriosis. Fertil Steril 2008.

the following cycling conditions: 94°C for 5 minutes followed by 30 cycles consisting of 94°C for 30 seconds, 63°C for 2 seconds, and 74°C for 20 seconds. This primer pair was designed to yield different product sizes for the *SV1*, *SV2*, *SV3*, and *SV4* mRNAs.

For *GHRH*, primers E1 and E4-1 (23) (0.25 μM each) were used for the primary amplification with the following cycling conditions: 94°C for 5 minutes followed by 30 cycles consisting of 94°C for 30 seconds, 64°C for 2 seconds, and 74°C for 10 seconds. We used 2 μL of the primary PCR product for the secondary PCR, using the primers E3 and E4-2 (24) (0.25 μM each) with the following cycling conditions: 94°C for 5 minutes followed by 25 cycles consisting of 94°C for 30 seconds, 62°C for 2 seconds, and 74°C for 5 seconds.

The secondary PCR products were analyzed by agarose gel electrophoresis and visualized by ethidium bromide. The RNA quality was tested by PCR amplification of human glyceraldehyde dehydrogenase (*GAPDH*) complementary DNA (cDNA) from the same RT reaction samples that were used for cDNA amplification of *GHRH* and *GHRH* SVs, as described earlier, using the control *GAPDH* primer set (Toyobo). An RT reaction without reverse transcriptase was used as a negative control.

Each PCR product was purified using the QIAEX II Gel Extraction Kit (Qiagen), and their sequence identities were confirmed using an ABI Prism 310 Genetic Analyzer (Applied Biosystems, Forster City, CA).

Treatment of ESC with hGHRH(1-29)NH2 to Study cAMP Response

To study the response of cAMP to exogenous GHRH, ESC were plated into a 24-well culture plate at 10^5 cells per well in 500 μL DMEM/F12 medium containing 10% FBS. When the cells had reached 80% confluence, they underwent serum starvation for 48 hours. Subsequently, the medium was replaced with 1% charcoal-stripped FBS medium containing 10^{-9} to 10^{-6} M hGHRH(1-29)NH_2 (Sigma) or vehicle with 50 μM isobutylmethylxanthine (IBMX), a cAMP phosphodiesterase inhibitor. We dissolved IBMX in 100% ethanol, and the final concentration of each vehicle in the medium was adjusted to 0.1%. Forskolin (10^{-7} M) was used as a positive control in each experiment.

After a 2-hour incubation (according to a preliminary experiment), conditioned media were collected, centrifuged, and stored at −80°C. Immediately after the conditioned media were collected, the wells were replenished with FBS-free medium so that the cell numbers could be counted using the Cell Counting Kit-8 (Dojindo, Kumamoto, Japan). Four separate experiments were done using tissues from four different women, and each experiment was performed in triplicate.

Measurement of cAMP Concentrations

The cAMP concentrations in aliquots of acetylated conditioned media were measured with a specific enzyme immunoassay (EIA) kit (Cayman Chemical Company, Ann Arbor,

MI), following the manufacturer's instructions. The cAMP concentrations were normalized to the cell counts in each corresponding well.

5-Bromo-2′-deoxyuridine (BrdU) Incorporation

The effect of GHRH on the proliferation of ESCs was evaluated by measuring the incorporation of 5-bromo-2′-deoxyuridine (BrdU) into cells. The incorporation of BrdU was detected using the Biotrak cell proliferation enzyme-linked immunosorbent assay (ELISA) system (Amersham Pharmacia Biotech), as reported previously elsewhere (25). Briefly, ESC were seeded into 96-multiwell Falcon plates at a density of 4000 cells per well in 100 μL of culture medium containing 10% FBS and were cultured for 48 hours, followed by a further 48 hours of serum starvation. After serum starvation, the medium was replaced with fresh medium supplemented with 1% charcoal-stripped FBS containing the control vehicle or hGHRH(1-29)NH_2 dissolved in dimethyl sulfoxide (DMSO) and diluted to 10^{-6} M with the medium. The final concentration of DMSO in the medium was 0.1%. Cells were incubated with 10 μL BrdU solution for the last 4 hours of the 24-hour and 48-hour culture periods. The culture medium was removed when the incubations had finished; the cells were fixed and the DNA was denatured by the addition of 200 μL fixative per well. The peroxidase-labeled anti-BrdU bound to the BrdU incorporated into newly synthesized cellular DNA. The immune complexes were detected by the subsequent substrate reaction, and the resultant color was read at 450 nm using the DigiScan Microplate Reader (ASYS Hitech GmbH, Eugendorf, Austria).

Statistical Analysis

The data were expressed as mean ± standard deviation. Student's *t*-test was used for paired comparisons and one-way analysis of variance (ANOVA), and a post hoc test was used for multiple comparisons using StatView software (SAS Institute Inc., Cary, NC). $P<.05$ was considered statistically significant.

RESULTS

Expression of GHRH and GHRH Receptor Splice Variant mRNA in Eutopic and Ectopic Endometrial Tissues

We performed RT-nested PCR to examine the mRNA expression of *GHRH* and the splice variants of the *GHRH* receptor in eutopic and ectopic endometrial tissues from 27 women with endometriosis, and eutopic endometrial tissues from 20 women without endometriosis (Fig. 1). The number of *GHRH*-positive samples was similar between ectopic endometrial tissues (24%) and eutopic endometrial tissues in patients with (26%) or without (25%) endometriosis (Table 2). We detected *SV1* mRNA in 63% of ectopic endometrial tissue samples, whereas expression was statistically significantly lower in eutopic endometrial tissues in patients with (none detected) or without (10%) endometriosis. We detected *GHRH* in all of the normal ovarian tissue samples (100%) used as controls, whereas *SV1* was not detected in any of these samples. Bands representing *SV2*, *SV3*, and *SV4* were not detected in any of the samples. In peritoneal bone marrow–derived cells, *GHRH* mRNA was detected in 7 out of 10 (70%) women with endometriosis and 6 out of 6 (100%) women without endometriosis.

Each PCR product was sequenced and confirmed to be identical to the *SV1* and *GHRH* sequences (14, 24).

FIGURE 1

Reverse transcriptase polymerase chain reaction analysis of the splice variants of the growth hormone–releasing hormone (GHRH) receptor and *GHRH* gene expression in eutopic and ectopic endometrial tissues. Data represent eutopic and ectopic endometrial tissues from 27 women with endometriosis, and eutopic endometrial tissues from 20 women without endometriosis. Amplification of GAPDH was performed to ensure equal loading. Lane M: 100-bp DNA molecular marker. Lanes 1–3: eutopic endometrial tissues from different patients without endometriosis. Lanes 4–6: eutopic endometrial tissues from different patients with endometriosis. Lanes 7–10: ectopic endometrial tissues from different patients.

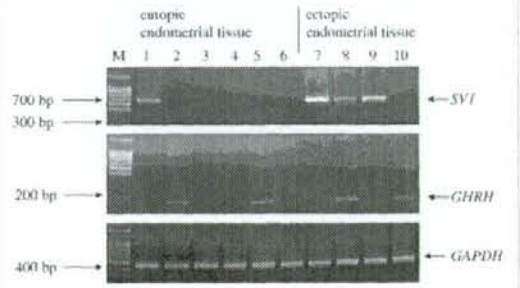

Fu. GHRH receptor SV1 in endometriosis. Fertil Steril 2008.

Effect of hGHRH(1-29)NH_2 on cAMP Production in ESC Expressing SV1

We first evaluated the expression of *SV1* mRNA in cultured ESC from 27 women. We detected *SV1* mRNA in 21 samples (77%), and the ESC that expressed *SV1* were used for the ensuing study. We evaluated the effect of hGHRH(1-29)NH_2 at concentrations between 10^{-9} M and 10^{-6} M on the production of cAMP. As shown in Figure 2, incubation with GHRH(1-29)NH_2 for 2 hours induced a dose-dependent increase in cAMP production in cultured ESC.

Effect of hGHRH(1-29)NH2 on DNA Synthesis in ESC

The effect of GHRH on DNA synthesis was examined in five independently cultured ESC preparations from five different

TABLE 2

Expression patterns of *GHRH* and *SV1* mRNA in three types of tissues.

	GHRH		SV1	
Tissue type	Rate	%	Rate	%
Endometriotic from ovarian endometrioma	6/27	24	17/27	63
Endometrial from women with endometriosis	7/27	26	0/27	0
Endometrial from women without endometriosis	5/20	25	2/20	10
Ovarian	14/14	100	0/14	0

Fu. GHRH receptor SV1 in endometriosis. Fertil Steril 2008.

women (Fig. 3). We found that hGHRH(1-29)NH_2 at a concentration of 10^{-7} M increased the incorporation of BrdU into DNA by 20% ($P<.05$) at 24 hours and 27% ($P<.05$) at 48 hours. At a concentration of 10^{-6} M, hGHRH(1-29)NH_2 increased BrdU incorporation by 23% ($P<.01$) at 24 hours and 33% ($P<.01$) at 48 hours. In contrast, hGHRH(1-29)NH_2 did not alter the amount of BrdU incorporated into the DNA of ESC that did not express *SV1* mRNA (data not shown, n = 3).

FIGURE 2

Effect of exogenous hGHRH(1-29)NH2 on cAMP production in cultured ectopic endometrial stromal cells (ESC). The cells were treated for 2 hours with hGHRH(1-29)NH2 (10^{-9} to 10^{-6} M) or forskolin (10^{-7} M). The cells were co-treated with isobutylmethylxanthine (IBMX) to suppress cAMP degradation. Conditioned media were assayed for cAMP concentration, and the cell numbers were determined using the Cell Counting Kit-8. Data represent the mean ± standard error of the mean of cAMP concentration per cell number of four separate experiments using different ESC preparations, expressed as a percentage of untreated controls. *$P<.05$ versus control.

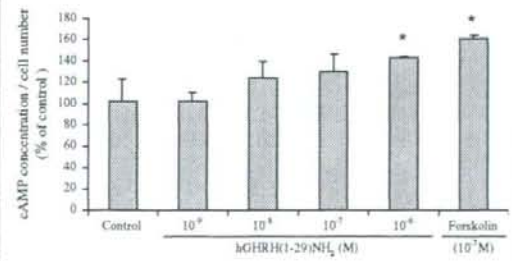

Fu. GHRH receptor SV1 in endometriosis. Fertil Steril 2008.

FIGURE 3

Effect of hGHRH(1-29)NH_2 on the proliferation of ectopic endometrial stromal cells (ESC) determined by BrdU incorporation using a cell proliferation ELISA system. The ESC were treated with hGHRH(1-29)NH_2 (10^{-7} M and 10^{-6} M) for 24 hours and 48 hours. Data represent the mean percentage of the untreated control ± standard error of the mean of five independent experiments using hexaplicate wells. *$P<.05$. **$P<.01$ versus control.

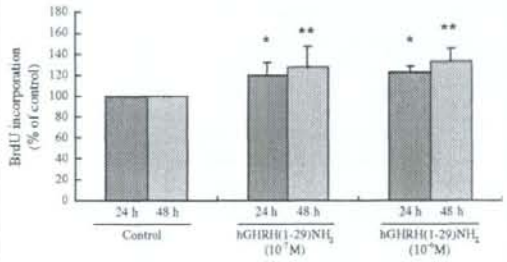

Fu. GHRH receptor SV1 in endometriosis. Fertil Steril 2008.

DISCUSSION

Our study demonstrated that *GHRH* receptor *SV1* mRNA was expressed in ESC. We also detected *GHRH* mRNA in eutopic and ectopic endometrium and in peritoneal bone marrow–derived cells. In addition, our results showed that GHRH stimulated cAMP production and cell proliferation in ESC expressing *SV1*.

The receptors mediating the possible actions of GHRH in extrapituitary tissues have only been identified recently. In initial tumor studies, the pituitary GHRH receptor could not be detected in any of the cancers studied (26, 27). However, recent investigations demonstrated that various human cancers express SVs of the GHRH receptor (8–12, 14, 28–30), and of these, SV1 displays the greatest sequence similarity to the pituitary GHRH receptor. It is now believed that the gene product of SV1 is a functional receptor that relays mitogenic and other signals in response to GHRH in tumors (11, 26, 27, 31).

Positive immunostaining of the GHRH receptor in the human endometrium has been reported recently (32). In our study, we could not detect gene expression of the pituitary GHRH receptor in any endometrial samples. The reason for the discrepancy between our data and the immunohistochemical study is unknown. Nevertheless, we have provided a remarkable finding with the detection of *SV1* mRNA in 17 out of 27 (63%) endometriotic samples and in 2 out of 49 (4%) eutopic endometrial samples. It is well established that the gene expression profile of the ectopic endometrium is different from that of the eutopic endometrium (1, 2). The higher expression rate of *SV1* in the ectopic endometrium may therefore indicate a higher sensitivity to GHRH in the ectopic endometrium.

The protein sequence encoded by SV1 is similar to that of the pituitary GHRH receptor, preserving the transmembrane domains, intracellular loops, and the C-terminal end necessary for signal transduction. However, the large N-terminal extracellular tail characteristic of the pituitary GHRH receptor is truncated (14). Functional differences between the activity of SV1 and the pituitary GHRH receptor are not clear at the moment. Several studies have shown that stimulation of SV1-transfected cells and SV1-expressing cells by GHRH or GHRH analogs is followed by an increase in cAMP production (8, 10, 13, 15, 33). Our study has revealed that SV1-expressing ESC respond to GHRH with a dose-dependent increase in cAMP production. Together with the finding that the ESC did not express the pituitary GHRH receptor (data not shown), the observed cAMP response to GHRH appears to be mediated by SV1.

Our study demonstrated that hGHRH(1-29)NH_2 increased DNA synthesis in ESC, as determined by BrdU incorporation. The observed effects of GHRH make an interesting contrast with GnRH II, which decreases DNA synthesis in ESC (16). It is intriguing to speculate that several hypothalamic hormones play different roles in endometriotic tissues. In addition, given that GHRH acts as a growth factor in ESC, the antiproliferative action of GHRH antagonists in various cancer cell lines (6) may be extrapolated to therapeutic potential in endometriosis.

We determined the expression rate of *GHRH* mRNA in normal human endometrial tissues and ectopic endometrial tissues. The rate of expression was very similar in eutopic endometrial samples from women with and without endometriosis and in ectopic endometrial samples, at approximately 25%. These expression rates are relatively low compared with those reported in prostate cancer (86%), endometrial cancer (68%), and ovarian cancer (55%) (12, 34). Although it is not yet known why this rate is lower, it is possible that endometrial tissue–derived GHRH might not act alone on SV1 in ESC. When GHRH is derived from other sources such as ovarian tissues and bone marrow–derived cells in the peritoneal cavity, it might also contribute to activating SV1 in the endometriotic cells.

Our study has demonstrated that SV1 is expressed in endometriotic stromal cells and that the activation of SV1 by GHRH stimulates the proliferation of these cells. These findings suggest that GHRH and SV1 are involved in the development of endometriosis.

Acknowledgments: The authors thank Emi Nose for her technical assistance, and our medical colleagues, especially Drs. Miyuki Harada, Tetsuya Hirata, Kaori Koga, Osamu Yoshino, Toshiki Tajima, Akiko Hasegawa, Kahori Hamasaki, Ako Kodama, and Hisahiko Hiroi, for their assistance.

REFERENCES

1. Matsuzaki S, Canis M, Pouly JL, Botchorishvili R, Dechelotte PJ, Mage G. Differential expression of genes in eutopic and ectopic endometrium from patients with ovarian endometriosis. Fertil Steril 2006;86:548–53.
2. Wu Y, Kajdacsy-Balla A, Strawn E, Basir Z, Halverson G, Jailwala P, et al. Transcriptional characterizations of differences between eutopic and ectopic endometrium. Endocrinology 2006;147:232–46.
3. Mayo KE, Miller T, DeAlmeida V, Godfrey P, Zheng J, Cunha SR. Regulation of the pituitary somatotroph cell by GHRH and its receptor. Recent Prog Horm Res 2000;55:237–66.
4. Kiaris H, Schally AV, Kalofoutis A. Extrapituitary effects of the growth hormone-releasing hormone. Vitam Horm 2005;70:1–24.
5. Kineman RD. Antitumorigenic actions of growth hormone-releasing hormone antagonists. Proc Natl Acad Sci USA 2000;97:532–4.
6. Schally AV, Varga JL. Antagonists of growth hormone-releasing hormone in oncology. Comb Chem High Throughput Screen 2006;9:163–70.
7. Schally AV, Comaru-Schally AM, Nagy A, Kovacs M, Szepeshazi K, Plonowski A, et al. Hypothalamic hormones and cancer. Front Neuroendocrinol 2001;22:248–91.
8. Busto R, Schally AV, Varga JL, Garcia-Fernandez MO, Groot K, Armatis P, et al. The expression of growth hormone-releasing hormone (GHRH) and splice variants of its receptor in human gastroenteropancreatic carcinomas. Proc Natl Acad Sci USA 2002;99:11866–71.
9. Busto R, Schally AV, Braczkowski R, Plonowski A, Krupa M, Groot K, et al. Expression of mRNA for growth hormone-releasing hormone and splice variants of GHRH receptors in human malignant bone tumors. Regul Pept 2002;108:47–53.
10. Garcia-Fernandez MO, Schally AV, Varga JL, Groot K, Busto R. The expression of growth hormone-releasing hormone (GHRH) and its receptor splice variants in human breast cancer lines; the evaluation of signaling mechanisms in the stimulation of cell proliferation. Breast Cancer Res Treat 2003;77:15–26.
11. Halmos G, Schally AV, Varga JL, Plonowski A, Rekasi Z, Czompoly T. Human renal cell carcinoma expresses distinct binding sites for growth hormone-releasing hormone. Proc Natl Acad Sci USA 2000;97:10555–60.
12. Halmos G, Schally AV, Czompoly T, Krupa M, Varga JL, Rekasi Z. Expression of growth hormone-releasing hormone and its receptor splice variants in human prostate cancer. J Clin Endocrinol Metab 2002;87:4707–14.
13. Kiaris H, Schally AV, Busto R, Halmos G, Artavanis-Tsakonas S, Varga JL. Expression of a splice variant of the receptor for GHRH in 3T3 fibroblasts activates cell proliferation responses to GHRH analogs. Proc Natl Acad Sci USA 2002;99:196–200.
14. Rekasi Z, Czompoly T, Schally AV, Halmos G. Isolation and sequencing of cDNAs for splice variants of growth hormone-releasing hormone receptors from human cancers. Proc Natl Acad Sci USA 2000;97:10561–6.
15. Rekasi Z, Varga JL, Schally AV, Plonowski A, Halmos G, Csernus B, et al. Antiproliferative actions of growth hormone-releasing hormone antagonists on MiaPaCa-2 human pancreatic cancer cells involve cAMP independent pathways. Peptides 2001;22:879–86.
16. Morimoto C, Osuga Y, Yano T, Takemura Y, Harada M, Hirata T, et al. GnRH II as a possible cytostatic regulator in the development of endometriosis. Hum Reprod 2005;20:3212–8.
17. Kempuraj D, Papadopoulou N, Stanford EJ, Christodoulou S, Madhappan B, Sant GR, et al. Increased numbers of activated mast cells in endometriosis lesions positive for corticotropin-releasing hormone and urocortin. Am J Reprod Immunol 2004;52:267–75.
18. Christodoulou C, Schally AV, Chatzistamou I, Kondi-Pafiti A, Lamnissou K, Kouloheri S, et al. Expression of growth hormone-releasing hormone (GHRH) and splice variant of GHRH receptors in normal mouse tissues. Regul Pept 2006;136:105–8.
19. Khorram O, Garthwaite M, Grosen E, Golos T. Human uterine and ovarian expression of growth hormone-releasing hormone messenger RNA in benign and malignant gynecologic conditions. Fertil Steril 2001;75:174–9.
20. Yoshino O, Osuga Y, Koga K, Hirota Y, Tsutsumi O, Yano T, et al. Concentrations of interferon-gamma–induced protein-10 (IP-10), an antiangiogenic substance, are decreased in peritoneal fluid of women with advanced endometriosis. Am J Reprod Immunol 2003;50:60–5.
21. Hirota Y, Osuga Y, Hirata T, Harada M, Morimoto C, Yoshino O, et al. Activation of protease-activated receptor 2 stimulates proliferation and

interleukin (IL)-6 and IL-8 secretion of endometriotic stromal cells. Hum Reprod 2005;20:3547–53.
22. Hirota Y, Osuga Y, Hirata T, Yoshino O, Koga K, Harada M, et al. Possible involvement of thrombin/protease-activated receptor 1 system in the pathogenesis of endometriosis. J Clin Endocrinol Metab 2005;90: 3673–9.
23. Kiaris H, Schally AV, Varga JL, Groot K, Armatis P. Growth hormone-releasing hormone: an autocrine growth factor for small cell lung carcinoma. Proc Natl Acad Sci USA 1999;96:14894–8.
24. Engel JB, Keller G, Schally AV, Toller GL, Groot K, Havt A, et al. Inhibition of growth of experimental human endometrial cancer by an antagonist of growth hormone-releasing hormone. J Clin Endocrinol Metab 2005;90:3614–21.
25. Tang X, Yano T, Osuga Y, Matsumi H, Yano N, Xu J, et al. Cellular mechanisms of growth inhibition of human epithelial ovarian cancer cell line by LH-releasing hormone antagonist Cetrorelix. J Clin Endocrinol Metab 2002;87:3721–7.
26. Kahan Z, Varga JL, Schally AV, Rekasi Z, Armatis P, Chatzistamou L, et al. Antagonists of growth hormone-releasing hormone arrest the growth of MDA-MB-468 estrogen-independent human breast cancers in nude mice. Breast Cancer Res Treat 2000;60:71–9.
27. Rekasi Z, Varga JL, Schally AV, Halmos G, Armatis P, Groot K, et al. Antagonists of growth hormone-releasing hormone and vasoactive intestinal peptide inhibit tumor proliferation by different mechanisms: evidence from in vitro studies on human prostatic and pancreatic cancers. Endocrinology 2000;141:2120–8.
28. Freddi S, Arnaldi G, Fazioli F, Scarpelli M, Appolloni G, Mancini T, et al. Expression of growth hormone-releasing hormone receptor splicing variants in human primary adrenocortical tumours. Clin Endocrinol (Oxf) 2005;62:533–8.
29. Havt A, Schally AV, Halmos G, Varga JL, Toller GL, Horvath JE, et al. The expression of the pituitary growth hormone-releasing hormone receptor and its splice variants in normal and neoplastic human tissues. Proc Natl Acad Sci USA 2005;102:17424–9.
30. Schulz S, Rocken C, Schulz S. Immunocytochemical localisation of plasma membrane GHRH receptors in human tumours using a novel anti-peptide antibody. Eur J Cancer 2006;42:2390–6.
31. Chatzistamou I, Schally AV, Varga JL, Groot K, Armatis P, Busto R, et al. Antagonists of growth hormone-releasing hormone and somatostatin analog RC-160 inhibit the growth of the OV-1063 human epithelial ovarian cancer cell line xenografted into nude mice. J Clin Endocrinol Metab 2001;86:2144–52.
32. Gallego R, Pintos E, Garcia-Caballero T, Raghay K, Boulanger L, Beiras A, et al. Cellular distribution of growth hormone-releasing hormone receptor in human reproductive system and breast and prostate cancers. Histol Histopathol 2005;20:697–706.
33. Rekasi Z, Varga JL, Schally AV, Halmos G, Groot K, Czompoly T. Antagonistic actions of analogs related to growth hormone-releasing hormone (GHRH) on receptors for GHRH and vasoactive intestinal peptide on rat pituitary and pineal cells in vitro. Proc Natl Acad Sci USA 2000;97: 1218–23.
34. Kahan Z, Arencibia JM, Csernus VJ, Groot K, Kineman RD, Robinson WR, et al. Expression of growth hormone-releasing hormone (GHRH) messenger ribonucleic acid and the presence of biologically active GHRH in human breast, endometrial, and ovarian cancers. J Clin Endocrinol Metab 1999;84:582–9.

Human Reproduction, Vol.24, No.2 pp. 408–414, 2009
Advanced Access publication on November 1, 2008 doi:10.1093/humrep/den385

human reproduction

ORIGINAL ARTICLE ***Reproductive biology***

Tunicamycin enhances the apoptosis induced by tumor necrosis factor-related apoptosis-inducing ligand in endometriotic stromal cells

Akiko Hasegawa, Yutaka Osuga[1], Yasushi Hirota, Kahori Hamasaki, Ako Kodama, Miyuki Harada, Toshiki Tajima, Yuri Takemura, Tetsuya Hirata, Osamu Yoshino, Kaori Koga, Tetsu Yano, and Yuji Taketani

Department of Obstetrics and Gynecology, Faculty of Medicine, University of Tokyo, 7-3-1, Hongo, Bunkyo-ku, Tokyo 113-8655, Japan

[1]Correspondence address. Tel: +81-3-3815-5411; Fax: +81-3-3816-2017; E-mail: yutakaos-tky@umin.ac.jp

TABLE OF CONTENTS

- Introduction
- Materials and Methods
- Results
- Discussion
- Acknowledgements
- Funding
- References

BACKGROUND: The increase in concentration of osteoprotegerin, an antagonist of tumor necrosis factor-related apoptosis-inducing ligand (TRAIL), in the peritoneal fluid of women with endometriosis may interfere with TRAIL-induced apoptosis in endometriotic cells and promote the development of endometriosis. In the present study, the effect of tunicamycin, a possible apoptosis enhancer, on TRAIL-induced apoptosis in endometriotic stromal cells (ESC) was determined.

METHODS: ESC were isolated from cyst walls of ovarian endometrioma and cultured. ESC were incubated with or without tunicamycin (2 μg/ml) for the first 16 h, and then incubated with or without TRAIL (200 ng/ml) for the following 24 h. To examine whether caspases were involved in TRAIL-induced apoptosis, z-VAD-fmk (30 μM), a general caspase inhibitor, was added 1 h before TRAIL treatment. ESC were transfected with small interfering RNA (siRNA) for DR5, a receptor of TRAIL, before tunicamycin treatment to evaluate its role in ESC. DR5 mRNA level was determined by quantitative RT–PCR. Apoptosis in ESC was evaluated by flow cytometry.

RESULTS: Tunicamycin increases both DR5 mRNA ($P < 0.005$) and TRAIL-induced apoptosis ($P < 0.0001$) in ESC. The increase in TRAIL-induced apoptosis in ESC by tunicamycin was suppressed ($P < 0.05$) by z-VAD-fmk. Transfection with DR5 siRNA suppressed the tunicamycin-induced increase in DR5 mRNA and abrogated the up-regulation of TRAIL-induced apoptosis by tunicamycin.

CONCLUSIONS: The combined treatment with tunicamycin and TRAIL may have therapeutic potential in the treatment of endometriosis.

Key words: endometriosis / apoptosis / tunicamycin / tumor necrosis factor-related apoptosis-induced ligand

Introduction

Endometriosis, defined by the presence of viable endometriotic tissue outside the uterus, is an enigmatic disease. It deteriorates the health of women of reproductive age, and there is no ideal therapeutic treatment for the disease due to a lack of knowledge of its etiology (Momoeda *et al.*, 2002; Osuga *et al.*, 2002). Implantation and growth of endometrial cells from the overflow of menstrual blood

into the peritoneal cavity is a widely accepted hypothesis for the pathogenesis of endometriosis. However, it is unclear why only a fraction of women develop endometriosis while retrograde menstruation is observed in most women.

Several lines of evidence indicate that a failure of apoptosis of ectopic and eutopic endometrial cells is a possible cause of endometriosis (Beliard *et al.*, 2004; Harada *et al.*, 2004b). Reduced apoptosis may be due to the decreased sensitivity of the endometrial and endometriotic cells to apoptotic stimuli, and/or impaired apoptotic stimuli to these cells in women with endometriosis. In this context, some studies have indicated that the concentration of osteoprotegerin (OPG) is elevated in the peritoneal fluid of women with endometriosis (Harada *et al.*, 2004a; Bersinger *et al.*, 2006). Since OPG has an antagonistic effect on tumor necrosis factor-related apoptosis-inducing ligand (TRAIL), TRAIL-induced endometriotic cell apoptosis may be attenuated, thereby allowing endometriosis to develop in these women.

Recently, enhancement of TRAIL-induced apoptosis by tunicamycin, via induction of endoplasmic reticulum (ER) stress, has been reported in colon and prostate cancer cells, and melanoma cells (Jin *et al.*, 2004; Shiraishi *et al.*, 2005; Jiang *et al.*, 2007). These studies suggest that tunicamycin-induced sensitization may be a promising strategy in cancer therapy. Meanwhile, the enhancement of TRAIL-induced apoptosis by tunicamycin might also be a unique therapy for endometriosis given that reduced apoptotic status of endometriotic cells contributes to the development of the disease. The current study investigates the effect of tunicamycin on endometriotic stromal cells (ESC), evaluating ER stress by mRNA expression of spliced XBP1 (sXBP1), a marker of ER stress (Ron and Walter, 2007), and apoptosis by flow cytometry analysis.

Materials and Methods

Reagents and materials

Type I collagenase, antibiotics (a mixture of penicillin, streptomycin and amphotericin B) and tunicamycin were purchased from Sigma (St Louis, MO, USA). Dulbecco's modified Eagle's medium (DMEM)/F-12 medium was obtained from Gibco (Grand Island, NY, USA). Charcoal-stripped fetal bovine serum (FBS) was from HyClone (Logan, UT, USA). Deoxyribonuclease I (DNase I), 0.25% Trypsin–EDTA, Lipofectamine RNAi max and Opti-MEM I were from Invitrogen (Carlsbad, CA, USA). TRAIL was purchased from Peprotech (Rocky Hill, NJ, USA). General caspase inhibitor Z-Val-Ala-Asp(OMe)-CH_2F (z-VAD-fmk) was purchased from Calbiochem (San Diego, CA, USA).

Sample collection

Endometriotic tissues were obtained from patients with ovarian endometriomas undergoing laparoscopy. Final diagnosis of ovarian endometrioma was confirmed by histopathological examination. Eutopic endometrial tissues were collected by curettage. Collected tissues were transported to the laboratory under sterile conditions and processed for the experiments. All women had regular menstrual cycles, and none had received hormonal treatment for at least 6 months before surgery. The institutional review board of the University of Tokyo approved the experimental procedures, and signed informed consent for the sample use was obtained from each patient.

Isolation and culture of ESC

The isolation and culturing of human ESC was performed as described previously (Hirota *et al.*, 2005a, c). Briefly, endometriotic tissues were minced into small pieces and incubated in DMEM/F12 containing type I collagenase (0.25%) and DNase I (15 IU/ml) for 2 h at 37°C. Dispersed endometriotic cells were separated by filtration through a 100-μm nylon cell strainer (BD Biosciences, Franklin Lakes, NJ, USA) and 70-μm nylon cell strainer. ESC in the filtrate were collected by centrifugation (250 g, 4 min, twice), resuspended in DMEM/F12 containing 5% FBS and antibiotics and plated onto 100-mm culture dishes (Iwaki, Tokyo, Japan). Dishes were kept at 37°C in a humidified 5% CO_2/95% air atmosphere for 1 or 2 days before the first passage. At the first passage, ESC were plated into 12-well plates at 1×10^5 cells/well for RT-PCR and small interfering RNA (siRNA) experiments, or 6-well plates at 4×10^5 cells/well for flow cytometry. The purity of ESC was more than 95%, according to positive cellular staining for vimentin (stromal cells) and negative cellular staining for cytokeratin (epithelial cells), CD45 (monocytes and other leukocytes) and von Willebrand factor (endothelial cells).

Treatment of ESC

When ESC reached 70–80% confluence in 1 or 2 days, media was removed and replaced with fresh media containing 1% charcoal-stripped FBS and antibiotics. After culturing for an additional 12 h, the cells were ready for use in the experiments. To see the effect of tunicamycin on mRNA levels of sXBP1, a marker of ER stress, ESC were incubated with 2 μg/ml tunicamycin for 0, 1, 3, 6 and 12 h. To examine the effect of tunicamycin on mRNA expression of DR5, a receptor of TRAIL, ESC were incubated with 2 μg/ml tunicamycin for 0, 1, 3, 6 and 12 h. For the each experiment, samples from three women were used. DR4, another TRAIL receptor, was not studied because its expression had not been detected in ESC (Harada *et al.*, 2004a). To see the effect of tunicamycin on TRAIL-induced apoptosis in ESC, ESC were incubated with or without tunicamycin (2 μg/ml) for the first 16 h, and then incubated with or without TRAIL (200 ng/ml) for the following 24 h. We selected the dose of TRAIL in reference to a recent study (Jiang *et al.*, 2007), whereas a lower dose (25 ng/ml) is used in another study (Shiraishi *et al.*, 2005). During the treatment, either the pan-caspase inhibitor z-VAD-fmk (30 μM), or a vehicle control was added 1 h before TRAIL treatment to examine whether caspases were involved in TRAIL-induced apoptosis in ESC. For this experiment, samples from two women were used.

Small interfering RNA

ESC seeded at 1×10^5 cells per well in 12-well plates 1 day before transfection reached 70–80% confluence on the day of transfection. The siRNA constructs used were obtained as ON-TARGET plus SMARTpool DR5 (L-004448-00-0005) from Dharmacon. The non-targeting siRNA control, ON-TARGET plus siCONTROL non-targeting pool (D-001810-10-05) was also obtained from Dharmacon. Cells were transfected with 50 nmol/l siRNA for 24 h in Opti-MEM I with 5% FBS media using Lipofectamine RNAi max according to the manufacturer's protocol. After transfection, media were removed and replaced with fresh media containing 1% charcoal-stripped FBS and antibiotics. After incubation for a further 12 h, cells were treated with tunicamycin and TRAIL as described above. For this experiment, samples from three women were used.

RNA extraction and real-time quantitative PCR

Total RNA was extracted from cultured ESC using the RNeasy Mini Kit (Qiagen, Hilden, Germany). Total RNA was extracted from eight

samples of eutopic endometrial tissues and eight samples of endometriotic tissues by the acid guanidinium–phenol–chloroform method using Isogen (Nippongene, Toyama, Japan). One microgram of total RNA was reverse transcribed in a 20 μl volume using Rever Tra Ace (TOYOBO, Osaka, Japan) according to the manufacturer's instructions. Real-time quantitative PCR was performed as previously reported (Hirata *et al.*, 2008) to assess sXBP1 and DR5 mRNA, and data analyses were performed using a Light Cycler (Roche Applied Science, Mannheim, Germany). sXBP1 and DR5 mRNA levels were normalized to RNA loading for each sample using glyceraldehyde-3-phosphate dehydrogenase (GAPDH) mRNA as an internal standard. PCR primers were purchased from TOYOBO and are as follows: sXBP1 primers (sense, 5′-GAGTTAAGACAGCGCTTGGG-3′; antisense, 5′-ACTGGGCCTGCACCTGCTGCG-3′) amplify a 118 bp fragment; DR5 primers (sense, 5′-TGCAGCCGTAGTCTTGATT G-3′; antisense, 5′-GCACCAAGTCTGCAAAGTCA-3′) amplify a 389 bp fragment; GAPDH primers (sense, 5′-ACCACAGTCCATG CCATCAC-3′; antisense, 5′-TCCACCACCCTGTTGCTGTA-3′) amplify a 452 bp fragment. For real-time quantitative PCR, the conditions were as follows: for sXBP1, 28 cycles at 95°C for 10 s, 70°C for 10 s, 72°C for 5 s; for DR5, 28 cycles at 95°C for 10 s, 64°C for 10 s, 72°C for 16 s; for GAPDH, 25 cycles at 95°C for 10 s, 64°C for 10 s, 72°C for 18 s. All PCR experiments were followed by melting curve analysis. Each PCR product was purified with a Qiaex II gel extraction kit (Qiagen, Tokyo, Japan), and their identities were confirmed by DNA sequencing (ABI Prism 310 Genetic Analyzer; Perkin-Elmer Applied Biosystems, Foster City, CA, USA).

Flow cytometry

Flow cytometric analysis was performed as reported previously (Hirota *et al.*, 2006). Apoptosis of ESC was assessed by double staining [annexin V and propidium iodide (PI)] using the Annexin V-FITC Apoptosis detection kit I (BD Biosciences, San Jose, CA, USA) according to the manufacturer's instructions. Briefly, ESC were detached by 0.25% Trypsin–EDTA, washed twice with phosphate-buffered saline, and resuspended in 1 × Binding Buffer at a concentration of 1×10^6 cells/ml. One hundred microliters of each sample solution were transferred to a 5 ml culture tube, 5 μl of annexin V-FITC and 2 μl of PI were added and the tubes incubated for 15 min at room temperature in the dark. After incubation, 400 μl of 1 × Binding Buffer was added to each sample tube and the samples analyzed by FACS Calibur and Cell Quest Pro (BD Biosciences, San Jose, CA, USA). Annexin V positive cells were regarded as apoptotic cells.

Isolation, culture and treatment of eutopic endometrial cells

The isolation and culture of eutopic endometrial cells of women with endometriosis ($n = 4$) or without endometriosis ($n = 3$) were performed according to the method that we have been using (Harada *et al.*, 2005; Hirota *et al.*, 2005b; Takemura *et al.*, 2006). In the same way as the treatment of ESC, eutopic endometrial cells were incubated with or without tunicamycin (2 μg/ml) for the first 16 h, and then incubated with or without TRAIL (200 ng/ml) for the following 24 h in order to see the effect of tunicamycin on TRAIL-induced apoptosis in eutopic endometrial cells.

Statistical analysis

Data were evaluated using analysis of variance with *post hoc* analysis (Fisher's protected least significance) for multiple comparisons. $P < 0.05$ were considered statistically significant.

Results

As shown in Fig. 1, treatment of ESC with tunicamycin increased mRNA levels of sXBP1, with a maximal increase of 7.8-fold compared with the basal level observed at 6 h. Tunicamycin also increased the gene expression of DR5, which reached 3.7-fold higher levels compared with the basal level at 12 h (Fig. 2).

Fig. 3A depicts representative flow cytometry data of ESC that were untreated (control) or treated with tunicamycin followed by TRAIL, clearly indicating increased apoptosis in the treated ESC. As shown in Fig. 3B, the percentage of apoptotic cells in control ESC was 4.7%, and TRAIL alone did not increase apoptosis in ESC. In contrast, pretreatment of ESC with tunicamycin followed by TRAIL treatment significantly increased apoptosis to 74.6%, while the addition of z-VAD-fmk reduced it to 26.1%. When control ESC were treated with tunicamycin alone, the percentage of apoptotic cells appeared slightly increased (11.8%).

In view of these findings, it was speculated that the increase in apoptosis following treatment of ESC by tunicamycin and TRAIL was a result of a tunicamycin-induced increase in DR5 expression. Knockdown of DR5 expression using DR5 siRNA dramatically reduced DR5 mRNA levels in tunicamycin-stimulated ESC (Fig. 4A). Importantly, DR5 siRNA also inhibited the increase in TRAIL-induced apoptosis in tunicamycin-treated ESC, whereas negative control siRNA did not affect the TRAIL-induced increase in apoptosis (Fig. 4B and C).

Fig. 5 shows DR5 mRNA levels in eutopic endometrial tissues and endometriotic tissues of women with endometriosis. DR5 mRNA was

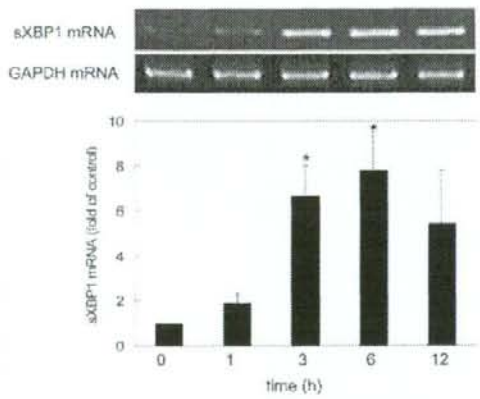

Figure 1 Tunicamycin-induced gene expression of sXBP1 in endometriotic stromal cells (ESC). ESC were cultured with tunicamycin for 0–12 h. Total RNA isolated from ESC was reverse transcribed, amplified by real-time PCR and representative amplified products are shown. The increase in levels of RNA was calculated by subtracting the signal threshold cycles of the internal standard (glyceraldehyde-3-phosphate dehydrogenase, GAPDH) from the threshold cycles of sXBP1. Values are the mean ± SEM of three independent experiments using samples from three different women. *$P < 0.05$ versus 0 h.

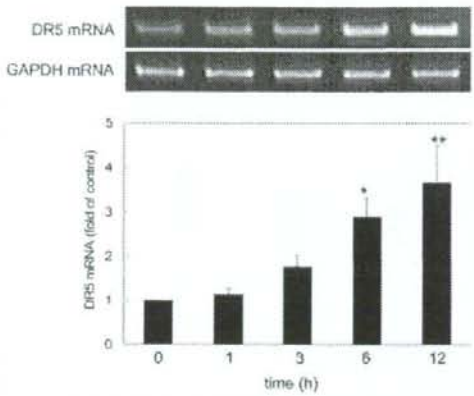

Figure 2 Tunicamycin-induced gene expression of DR5 in ESC. ESC were cultured with tunicamycin for 0–12 h and the same procedures as described in Fig. 1 were used to measure DR5 mRNA. Values are the mean ± SEM of three independent experiments using samples from three different women. $^{*}P < 0.05$; $^{**}P < 0.005$ (both versus 0 h).

at significantly higher levels in eutopic endometrial tissues than in endometriotic tissues.

In order to supplement the present study, we examined apoptosis induced by tunicamycin and TRAIL in eutopic endometrial cells of women with and without endometriosis (Table I). In eutopic endometrial cells of women without endometriosis, tunicamycin in combination with TRAIL showed no additive effect on tunicamycin alone, which induced an increase of apoptosis compared with the control. In eutopic endometrial cells of women with endometriosis, tunicamycin tended to increase TRAIL-induced apoptosis, though the increased levels seem to be quite low compared with those observed in ESC.

Discussion

The present study has demonstrated that the addition of tunicamycin to ESC increases the production of sXBP1 mRNA, a marker of ER stress, and the mRNA levels of DR5, a typical proapoptotic receptor of TRAIL. A substantial increase in apoptosis was observed upon the addition of TRAIL to ESC pretreated with tunicamycin, and apoptosis was significantly suppressed by the treatment of ESC with the general caspase inhibitor, as well as DR5 siRNA.

Reduced apoptosis of endometrial and/or endometriotic cells has been noted as a possible mechanism of the development of endometriosis. This implies that the induction of apoptosis in these cells may suppress the progress of the disease. GnRH analogues are currently widely used to treat endometriosis, and GnRH analogue-induced apoptosis of endometriotic cells has been observed *in vivo* and *in vitro* (Imai *et al.*, 2000; Meresman *et al.*, 2003). However, GnRH analogue treatment has various serious side effects, such as inducing a hypoestrogen state in the patient, and alternative treatment that does not affect the hormonal status of the patient is required.

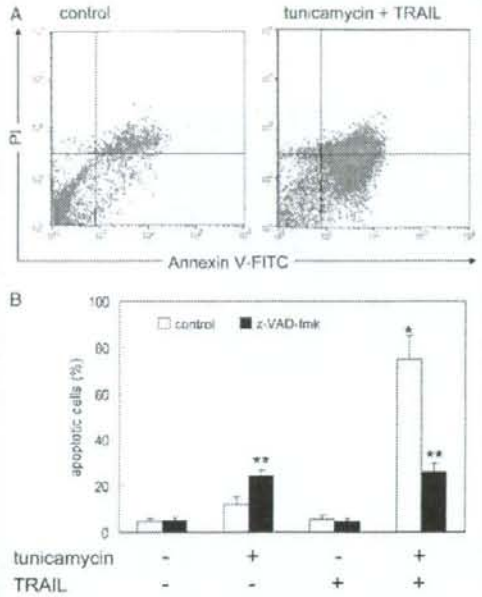

Figure 3 Effect of tumor necrosis factor-related apoptosis-induced ligand (TRAIL) on apoptosis of ESC with or without tunicamycin pretreatment, and effect of a general caspase inhibitor, z-VAD-fmk, on the TRAIL-induced apoptosis. ESC were cultured with or without tunicamycin (2 μg/ml) for 16 h, then treated with or without TRAIL (200 ng/ml) for 24 h. One hour before TRAIL treatment, z-VAD-fmk or the control vehicle was added to the culture. Apoptosis was analyzed by flow cytometry on 5×10^4 ESC that were double stained [annexin V and propidium iodide (PI)]. Annexin V-positive cells, both dead and live, were regarded as apoptotic cells. (**A**) The representative flow cytometry data. (**B**) Percentage of apoptotic cells in each treatment. Values are the mean ± SEM of two independent experiments using samples from two different women. $^{*}P < 0.0001$ versus all others; $^{**}P < 0.05$ versus all tunicamycin (−) groups. FITC, fluorescein isothiocyanate.

Recent studies have identified compounds that regulate apoptosis in ESC, and several of these increase apoptosis of endometriotic cells. Their usefulness for endometriosis therapy is currently being evaluated (Nasu *et al.*, 2005, 2007; Wang *et al.*, 2005).

The present study has demonstrated that tunicamycin has distinctive characteristics among the drugs that induce apoptosis of endometriotic cells. Given that the peritoneal environment of endometriotic women interferes with the proapoptotic function of TRAIL, as shown by the increase in OPG concentrations (Harada *et al.* 2004a; Bersinger *et al.*, 2006) and the resultant decrease in TRAIL/OPG ratio in the peritoneal fluid of endometriotic women, an agent that sensitizes endometriotic cells to TRAIL-induced apoptosis could be highly effective for the treatment of endometriosis. Tunicamycin, in combination with TRAIL, may be that agent since it substantially increased apoptosis in ESC. The combined treatment with

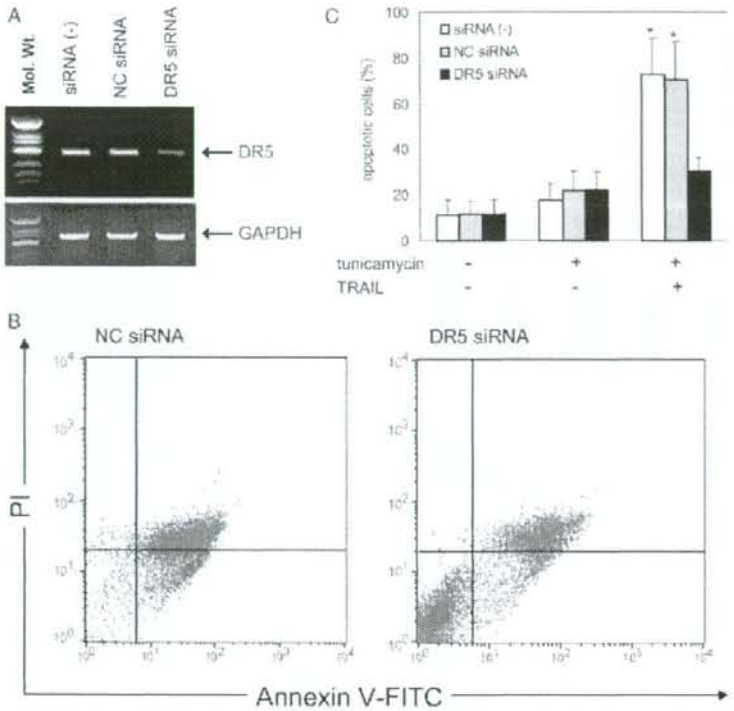

Figure 4 Effect of DR5 small interfering RNA (siRNA) on TRAIL-induced apoptosis of ESC pretreated with tunicamycin. First, ESC were transfected with the control, or DR5 siRNA for 24 h [siRNA (−), mock transfection; NC siRNA, negative control siRNA transfection; DR siRNA, DR siRNA transfection]. Subsequently, ESC were cultured with or without tunicamycin (2 μg/ml) for 16 h, followed by treatment with or without TRAIL (200 ng/ml) for 24 h. Apoptosis of ESC was analyzed by flow cytometry on 5×10^4 ESC that were double stained (annexin V and PI). Annexin V-positive cells, both dead and live, were regarded as apoptotic cells. (**A**) DR5 mRNA in ESC after tunicamycin treatment for 16 h. Amplification of GAPDH was used as a reference for determining RNA quality and amounts. (**B**) Representative flow cytometry data of ESC after treatment with TRAIL for 24 h. (**C**) Percentage of apoptotic cells after each treatment. Values are the mean ± SEM of three independent experiments using samples from three different women. *$P < 0.005$ versus all others.

tunicamycin and TRAIL may have therapeutic potential in the treatment of endometriosis. However, careful evaluation of low doses of tunicamycin in combination with TRAIL is required before *in vivo* investigations are carried out because tunicamycin induces varying degrees of apoptosis in normal cells, such as melanocytes, fibroblasts and human umbilical venous endothelial cells (Jiang *et al.*, 2007).

Endometriotic tissues are in a state of low apoptosis (Harada *et al.*, 2004b) and are generally resistant to drug-induced apoptosis (Izawa *et al.*, 2006). In light of a genome-wide study which showed that proapoptotic genes are down-regulated in endometriotic tissues as compared with eutopic endometrial tissues (Arimoto *et al.*, 2003), genetic differences between endometriotic cells and eutopic endometrial cells may contribute to the resistance of the former to apoptosis. In this context, decreased levels of DR5 mRNA in endometriotic tissues compared with eutopic endometrial tissues is a notable finding, and up-regulation of DR5 by tunicamycin may be a reasonable approach to sensitizing ESC to apoptotic stimulation by TRAIL.

Tunicamycin is a typical inducer of ER stress, a cellular stress response to perturbations in the protein folding functionality of the ER (Xu *et al.*, 2005). ER stress activates the unfolded protein response, which is mediated by the activation of three signal transduction cascades originating from the three ER transmembrane proteins PERK, ATF6 and IRE1. Activated IRE1 splices XBP1 to produce sXBP1. In this study, the tunicamycin-induced increase of sXBP1 mRNA in ESC indicates enhanced ER stress and activation of IRE1. A recent study has shown that suppression of the IRE1 signal transduction pathway inhibited tunicamycin-induced up-regulation of DR5 in one melanoma cell line but not in another melanoma cell line, implying a diversity of pathways regulating tunicamycin-induced DR5 expression (Jiang *et al.*, 2007). We have also shown that knockdown of IRE1 using siRNA inhibited the increase of sXBP1, but did not suppress the increased expression of DR5 and the increased apoptosis in ESC (data not shown). Tunicamycin-induced up-regulation of DR5 in ESC appears to be mediated by a pathway other than the IRE1 pathway.